Evidence for fire in the Pliocene Arctic in response to amplified temperature

Tamara Fletcher[1*], Lisa Warden[2*], Jaap S. Sinninghe Damsté[2,3], Kendrick J. Brown[4,5], Natalia Rybczynski[6,7], John Gosse[8], and Ashley P Ballantyne[1]

[1] College of Forestry and Conservation, University of Montana, Missoula, 59812, USA
[2] Department of Marine Microbiology and Biogeochemistry, NIOZ Royal Netherlands Institute for Sea Research, Den Berg, 1790, Netherlands
[3] Department of Earth Sciences, University of Utrecht, Utrecht, 3508, Netherlands
[4] Natural Resources Canada, Canadian Forest Service, Victoria, V8Z 1M, Canada
[5] Department of Earth, Environmental and Geographic Science, University of British Columbia Okanagan, Kelowna, V1V 1V7, Canada
[6] Department of Palaeobiology, Canadian Museum of Nature, Ottawa, K1P 6P4, Canada
[7] Department of Biology & Department of Earth Sciences, Carleton University, Ottawa, K1S 5B6, Canada
[8] Department of Earth Sciences, Dalhousie University, Halifax, B3H 4R2, Canada
*Authors contributed equally to this work

Correspondence to: Tamara Fletcher (tamara.fletcher@umontana.edu)

Abstract. The mid-Pliocene is a valuable time interval for investigating equilibrium climate at current atmospheric CO_2 concentrations, because atmospheric CO_2 concentrations are thought to have been comparable to current day and yet the climate and distribution of ecosystems was quite different. One intriguing, but not fully understood, feature of the early to mid-Pliocene climate is the amplified arctic temperature response and its impact on arctic ecosystems. Current models underestimate the degree of warming in the Pliocene Arctic and validation of proposed feedbacks is limited by scarce terrestrial records of climate and environment. Here we reconstruct the summer temperature and fire regime from a sub-fossil fen-peat deposit on west-central Ellesmere Island, Canada, that has been chronologically constrained using radionuclide dating to 3.9 +1.5/-0.5 Ma.

The estimate for average mean summer temperature is 15.4±0.8°C using specific bacterial membrane lipids, i.e. branched glycerol dialkyl glycerol tetraethers. Macro-charcoal was present in all samples from this Pliocene section with notably higher charcoal concentration in the upper part of the sequence. This change in charcoal was synchronous with a change in vegetation that saw fire-promoting *Pinus* and *Picea* increase in abundance. Paleovegetation reconstructions are consistent with warm summer temperatures, relatively low summer precipitation and an incidence of fire comparable to fire adapted boreal forests of North America, or potentially central Siberia.

To our knowledge, this site provides the northern-most evidence of fire during the Pliocene. It suggests that ecosystem productivity was much greater, providing fuel for wildfires, and that the climate was conducive to the ignition of fire during this period. This study indicates that interactions between paleovegetation and paleoclimate were mediated by fire in the High Arctic during the Pliocene, even though CO_2 concentrations were similar to modern.

1 Introduction

Current rates of warming in the Canadian Arctic are now roughly triple the rate of global warming (Bush and Lemmen, 2019). Since 1850, global land surface temperatures have increased by approximately 1.0°C, whereas circum-arctic

land surface temperatures have increased by >2.0°C (Jones and Moberg, 2003; Francis and Skific, 2015). Such arctic amplification of temperatures has also occurred during other warm climate anomalies in Earth's past. Paleoclimate records from the Arctic indicate that the change in arctic summer temperatures during past global warm periods was 3–4 times larger than global temperature change (Miller et al., 2010). While the latest ensemble of earth system models (ESMs) provide fairly accurate predictions of the modern amplification of arctic temperatures hitherto observed (Marshall et al., 2014), they often under-predict the amplification of arctic temperatures during past warm intervals in Earth's history, including the Eocene (33.9–56 Ma; Shellito et al., 2009), and the Pliocene (2.6–5.3 Ma; Dowsett et al., 2012; Salzmann et al., 2013) epochs. These differences suggest that either the models are not simulating the full array of feedback mechanisms properly for past climates, or that the full array of fast and slow feedback mechanisms have not manifested for the modern Arctic. If the later, the Arctic region and its ecosystems have yet to reach a new equilibrium in response to full temperature amplification.

The Pliocene is an intriguing climatic interval that may offer important insights into climate feedbacks. Atmospheric CO_2 concentrations were, at times, as high as modern (Fig. 1), but generally show a decreasing trend throughout the Pliocene (Haywood et al., 2016; Pagani et al., 2010; Royer et al., 2007; Stap et al., 2016),. Although CO_2 estimates from different methods do not converge, the modelled direct effects of these CO_2 discrepancies appear to be small (Feng et al., 2017). Of additional importance for comparability to the modern climate system, continental configurations were similar to present (Dowsett et al., 2016). While global mean annual temperatures (MATs) during the Pliocene were only ~ 3°C warmer than present day, arctic land surface MATs may have been as much as 15 to 22°C warmer (Ballantyne et al., 2010; Csank et al., 2011a; Csank et al., 2011b; Fletcher et al., 2017). Further, arctic sea surface temperatures may have been as much as 10 to 15°C warmer than modern (Robinson, 2009), and sea-levels were approximately 25m higher than present (Dowsett et al., 2016). As a result, the Arctic terrestrial environment was significantly different from today, with boreal ecosystems at much higher latitudes (Salzmann et al., 2008). These changes in vegetation due to climate, may have also provided further important feedbacks to arctic temperatures (e.g. Otto-Bliesner and Upchurch Jr, 1997).

To advance our understanding of arctic ecosystem response and feedback to temperature amplification during past warm intervals in Earth's history this investigation targets an exceptionally well-preserved arctic sedimentary sequence to simultaneously reconstruct summer temperature, vegetation and fire from a single site.

2 Methods

2.1 Site description

To investigate the environment and climate of the Pliocene Arctic we focused on the Beaver Pond (BP) fossil site, located at 78° 33′ N (Fig. 2) on Ellesmere Island. The stratigraphic section located at ~380 meters above sea level (MASL) today includes unconsolidated bedded sands and gravels, and rich organic layers including a fossil rich peat layer, up to 2.4 m thick, with sticks gnawed by an extinct beaver (*Dipoides spp.*). The assemblage of fossil plants and animals at BP has been studied extensively to gain insight into the past climate and ecology of the Canadian High Arctic (Ballantyne et al., 2006; Csank et al., 2011a; Csank et al., 2011b; Fletcher et al., 2017; Mitchell et al., 2016;

Rybczynski et al., 2013; Tedford and Harington, 2003; Wang et al., 2017). Previous paleoenvironmental evidence suggests the main peat unit is a rich fen deposit with a neutral to alkaline pH, associated with open water (Mitchell et al., 2016), likely a lake edge fen or shallow lake fen, within a larch-dominated forest-tundra environment (Matthews and Fyles, 2000), not a low pH peat-bog. While the larch species identified at the site, *Larix groenlandia*, is extinct (Matthews and Fyles, 2000), many other plant remains are Pliocene examples of taxa that are extant (Fletcher et al., 2017).

The fen-peat unit examined in this study was sampled in 2006 and 2010. The main sequence examined across the methods used in this study includes material from Unit II, the entire span of Unit III, and material from Unit IV sampled from Section A as per Mitchell et al. (2016; Fig. S1; see Mitchell et al. 2016 Fig 5), with a total sampled profile of 1.65 m. Unit III has been estimated to represent ~20 000 years of deposition based on modern northern fen accumulation rates (Mitchell et al., 2016). The charcoal estimates from this locality were based on 31 sample layers from the 2006 field campaign, while the temperature estimates from specific bacterial membrane lipids were taken from 22 of the sample layers collected in 2006 and an additional 12 samples collected in 2010. The same samples from the 2006 season were analyzed for mean summer temperature and char count where contents of the sample allowed. Pollen was tabulated from 10 samples from the 2006 sequence, located at different stratigraphic depths.

2.2 Geochronology

While direct dating of the peat was not possible, we were able to establish a burial age for fluvial sediments deposited approximately 4–5 m above and 30 m to the southwest of the peat. We used a method based on the ratio of isotopes produced in quartz by secondary cosmic rays. The cosmogenic nuclide burial dating approach measures the ratio of cosmogenic ^{26}Al ($t_{½}$ = 0.71 Ma) and ^{10}Be ($t_{½}$ = 1.38 Ma) in quartz sand grains that were exposed on hillslopes and alluvium prior to final deposition at BP. Once the quartz grains are completely shielded from cosmic rays, the ratio of the pair will predictably decrease because ^{26}Al has double the radiodecay rate of ^{10}Be. In 2008, four of the medium to coarse grained quartz samples were collected from a vertical profile of planar crossbedded fluvial sands between 8.7 and 10.4 m below the overlying till surface. The samples were 5 cm thick, separated by an average of 62 cm, and should closely date the peat (the sandy braided stream beds represent on the order of ~10^4 years from the top of the peat to the highest sample). Quartz concentrates were extracted from the arkosic sediment using Frantz magnetic separation, heavy liquids, and differential leaching with HF in ultrasonic baths. When sample aliquots reached aluminum concentrations <100 ppm (ICP-OES) as a proxy of feldspar abundance, the quartz concentrate was subjected to a series of HF digestion and rinsing steps to ensure that more than 30% of the quartz had been dissolved to remove meteoric ^{10}Be. Approximately 200 mg of Be extracted from a Homestake Gold Mine beryl-based carrier was added to 150 g of each quartz concentrate (no Al carrier was needed for these samples). Such large quartz masses were digested because of the uncertainty in the abundance of the faster decaying isotope. Following repeated perchloric-acid dry-downs to remove unreacted HF, pH-controlled precipitation, column chemistry ion chromatography to extract the Be and Al ions, precipitation in ultrapure ammonia gas, and calcination at temperatures above 1000°C in a Bunsen flame for three minutes, oxides were mixed with equal amounts of niobium and silver by volume. These were packed into stainless steel targets for measurement at Lawrence Livermore National Laboratory's

accelerator mass spectrometer (AMS). Uncertainty estimates for $^{26}Al/^{10}Be$ were calculated as 1σ by combining AMS precision with geochemistry errors in quadrature. For a complete detailed description of TCN methods see Rybczynski et al. (2013). The ages provided here are updated from Rybczynski et al. (2013) by using more recent production rate information and considering the potential for increasing exposure to deeply penetrating muons during the natural post-burial exhumation at BP.

2.3 Paleotemperature Reconstruction

Paleotemperature estimates were determined based on the distribution of fossilized, sedimentary membrane lipids known as branched glycerol dialkyl glycerol tetraethers (brGDGTs) that are well preserved in peat bogs, soils, and lakes (Powers et al., 2004; Weijers et al., 2007c). These unique lipids are thought to be synthesized by a wide array of Acidobacteria within the soil (Sinninghe Damsté et al., 2011; Sinninghe Damsté et al., 2014) and presumably other bacteria (Sinninghe Damsté et al., 2018) in soils and peat bogs but also in aquatic systems. Previously, it has been established that the degree of methyl branching (expressed in the methylation index of branched tetraethers; MBT) is correlated with mean annual air temperature (MAAT), and the relative amount of cyclopentane moieties (expressed in the cyclization index of branched tetraethers; CBT) has been shown to correlate with both soil pH and MAAT (Weijers et al., 2007b). Because of the relationship of the distribution of these fossilized membrane lipids with these environmental parameters, it has been used for paleoclimate applications in different environments including coastal marine sediments (Bendle et al., 2010; Weijers et al., 2007a), peats (Ballantyne et al., 2010; Naafs et al., 2017), paleosols (Peterse et al., 2011; Zech et al., 2012), and lacustrine sediments (Loomis et al., 2012; Niemann et al., 2012; Pearson et al., 2011; Zink et al., 2010). In this study we reconstruct mean summer air temperature (MST), using a modified version of a calibration that was developed by Pearson et al. (2011) and is based on 90 core top lacustrine sediment samples from diverse climates and geographical areas.

Improved separation methods (Hopmans et al., 2016) have recently led to the separation and quantification of the 5- and 6-methyl brGDGT isomers that used to be treated as one since the 6-methyl isomers were co-eluting with the 5-methyl isomers (De Jonge et al., 2013). This has led to the definition of new indices and improved MAAT calibrations based on the global soil (De Jonge et al., 2014), peat (Naafs et al., 2017), and African lake (Russell et al., 2018) datasets.

Sediment samples were freeze-dried and then ground and homogenized with a mortar and pestle. Next, using the Dionex™ accelerated solvent extractor (ASE), 0.5–1.0 g of sediment was extracted with the solvent mixture of dichloromethane (DCM):methanol (9:1, v/v) at a temperature of 100°C and a pressure of 1500 psi (5 min each) with 60% flush and purge 60 s. The Caliper Turbovap®LV was utilized to concentrate the collected extract, which was then transferred using DCM and dried over anhydrous Na_2SO_4 before being concentrated again under a gentle stream of N_2 gas. To quantify the amount of GDGTs, 1 µg of an internal standard (C46 GDGT; Huguet et al., 2006) was added to the total lipid extract. Then, the total lipid extract was separated into three fractions using hexane:DCM (9:1, v:v) for the apolar fraction, hexane:DCM (1:1, v:v) for the ketone fraction and DCM:MeOH (1:1, v:v) for the polar fraction, using a column composed of Al_2O_3, which was activated for 2 h at 150°C. The polar fraction, which contained the GDGTs, was dried under a steady stream of N_2 gas and weighed before being re-dissolved in hexane:isopropoanol

(99:1, v:v) at a concentration of 10 mg ml^{-1} and subsequently passed through a 0.45 μm PTFE filter. Finally, the polar fractions were analyzed for GDGTs by ultra-high performance liquid chromatography – atmospheric pressure positive ion chemical ionization – mass spectrometry (UHPLC-APCI-MS) using the method described by Hopmans et al., (2016). The polar fractions of some samples were re-run on the UHPLC-APCI-MS multiple times and the average fractional abundances of the brGDGTs was determined.

For the calculation of brGDGT-based proxies, the brGDGTs are specified by the Roman numerals as indicated in Fig. S2. The 6-methyl brGDGTs are distinguished from the 5-methyl brGDGTs by a prime. The novel indices, including MBT'_{5Me} based on just the 5-methyl brGDGTs and the CBT′ that was used to calculate the pH (De Jonge et al., 2014):

$$MBT'_{5Me} = ([Ia] + [Ib] + [Ic]) / ([Ia] + [Ib] + [Ic] + [IIa] + [IIb] + [IIc] + [IIIa] + [IIIb] + [IIIc]) \quad (1)$$

$$CBT' = -^{10}\log[([Ic] + [IIa'] + [IIb'] + [IIc'] + [IIIa'] + [IIIb'] + [IIIc'])/([Ia] + [IIa] + [IIIa])] \quad (2)$$

The square brackets denote the fractional abundance of the brGDGT within the bracket relative to the total brGDGTs. The distributions of aquatically produced brGDGTs in the lake calibration developed by Pearson et al. (2011) were used to determine MST. When this calibration is used the fractional abundances of IIa and IIa′ must be summed because these two isomers co-eluted under the chromatographic conditions used by Pearson et al. (2011):

$$MST\ (°C) = 20.9 + 98.1 \times [Ib] - 12 \times ([IIa] + [IIa']) - 20.5 \times [IIIa] \quad RMSE = 2.0°C \quad (3)$$

MAAT and surface water pH were also calculated using a novel calibration created using sediments from East African lakes analysed with the novel chromatography method and based upon MBT'_{5Me} (Russell et al., 2018).

$$MAAT = -1.2141 + 32.4223 * MBT'_{5Me} \quad RMSE\ of\ 2.44\ °C \quad (4)$$

$$Surface\ water\ pH = 8.95 + 2.65 * CBT' \quad RMSE\ of\ 0.80 \quad (5)$$

2.4 Vegetation and Fire Reconstruction

For charcoal, a total of thirty 2 cm^3 samples were taken at 5 cm intervals from depths from 380 and 381.45 MASL at the BP site, with an additional 2cm^{-3} sample collected at 381.65 MASL. All samples were deflocculated using sodium hexametaphosphate and passed through 500, 250 and 125 μm nested mesh sieves. The residual sample caught on each sieve was then collected in a gridded petri dish and examined using a stereomicroscope at 20-40X magnification to obtain charcoal concentration (fragments cm^{-3}). Charcoal area (mm^2 cm^{-3}) was measured for each sample using specialized imaging software from Scion Corporation. For a detailed description of methods see Brown and Power (2013).

Vegetation was reconstructed using pollen and spores (herein pollen) at selected elevations chosen to capture upper and lower sections of the elevation profile, and that corresponded with changes in charcoal. The sample depths selected for pollen analyses were 380.3–380.4 MASL, 381.10–381.25 MASL, and 381.35–381.45 MASL. Samples were

processed using standard approaches (Moore et al., 1991), whereby 1cm^3 sediment subsamples were treated with 5% KOH to remove humic acids and break up the samples. Carbonates were dissolved using 10% HCl, whereas silicates and organics were removed by HF and acetolysis treatment, respectively. Pollen slides were made by homogenizing 35 µl of residue, measured using a single-channel pipette, with 15 µl of melted glycerin jelly. Slides were counted using a Leica DM4000 B LED compound microscope at 400–630x magnification. A reference collection and published keys (McAndrews et al., 1973; Moore et al., 1991) aided identification.

In addition to tabulating pollen and charcoal, a list of plant taxa derived from Beaver Pond was previously compiled in Fletcher et al. (2017). Extant species from this list were selected and their modern occurrences extracted from the Global Biodiversity Information Facility (GBIF.org, 2017). Observation data was grouped by 5° latitude 5° longitude grids cells, and the shared species count calculated using R (R Core Team, 2016). Modern fire frequency was mapped using the MODIS 6 Active Fire Product. The fire pixel detection count per day, within the same 5° latitude 5° longitude grids cells was counted over the ten years 2006–2015, and standardized by area of the cell. The modern climate maps were generated using data from WorldClim 1.4 (Hijmans et al., 2005). The values for the bioclimatic variables mean temperature of the warmest quarter (equivalent to MST) and precipitation of the warmest quarter (summer precipitation) were also averaged by grid cell. The shared species count, climate values, and fire day detections were mapped to the northern polar stereographic projection in ArcMap 10.1.

3 Results

3.1 Geochronology

The burial dating results with $^{26}Al/^{10}Be$ in quartz sand at 10 m below modern depth provides four individual ages. From shallowest to deepest, the burial ages are 3.6 +1.5/-0.5 Ma, 3.9 +3.7/-0.5 Ma, 4.1 +5.8/-0.4 Ma, and 4.0 +1.5/-0.4 Ma (Table S2), with an unweighted mean age of 3.9 Ma. The convoluted probability distribution function yields a maximum probability age of 4.5 Ma. Unfortunately, the positive tails of the probability distribution functions of two of the samples exceeds the radiodecay saturation limit of the burial age. Therefore, their probability distributions do not reflect the actual age probabilities and uncertainty. Given the positive tail in the probability distribution functions, and the inability to convolve all samples, we recommend using the unweighted mean age, 3.9 Ma, with an uncertainty of +1.5/-0.5 Ma as indicated by the two samples with unsaturated limits. Despite the apparent upward younging of the individual burial ages, the 1σ-uncertainties overlap rendering the samples indistinguishable.

3.2 Paleotemperature Estimates

3.2.1 Provenance of branched GDGTs

Previously, brGDGT derived MAAT estimates (-0.6 ± 5.0 °C) from BP sediments were developed using the older chromatography methods that did not separate the 5- and 6- methyl brGDGTs, and a soil calibration (Ballantyne et al., 2010). In marine and lacustrine sediments, bacterial brGDGTs were thought to originate predominantly from continental soil erosion arriving in the sediments through terrestrial runoff. More recent studies, however, have indicated aquatically produced brGDGTs could be affecting the distribution of the sedimentary brGDGTs and thus

the temperature estimates based upon them (Warden et al., 2016; Zell et al., 2013; Zhu et al., 2011). Since the discovery that sedimentary brGDGTs can have varying sources, different calibrations have been developed depending on the origin of the brGDGTs, i.e. soil calibration (De Jonge et al., 2014), peat calibration (Naafs et al., 2017) and aquatic calibrations (i.e. Foster et al., 2016; Pearson et al., 2011; Russell et al., 2018). Therefore, several studies have recommended that the potential sources of the sedimentary brGDGTs should be investigated before attempting to use brGDGTs for paleoclimate applications (De Jonge et al., 2015; Warden et al., 2016; Yang et al., 2013; Zell et al., 2013). In this study, we examine the distribution of brGDGTs in an attempt to determine their origin and consequently the most appropriate calibration to utilize in order to reconstruct temperatures from the BP sediments.

Branched GDGTs IIIa and IIIa′ on average had the highest fractional abundance of the brGDGTs detected in the BP sediments (see Fig. S2 for structures; Table S4). A previous study established that when plotted in a ternary diagram the fractional abundances of the tetra-, penta- and hexamethylated brGDGTs, soils lie within a distinct area (Sinninghe Damsté, 2016). To assess whether the brGDGTs in the BP deposit were predominantly derived from soils, we compared the fractional abundances of the tetra-, penta- and hexamethylated brGDGTs in the BP sediments to those from modern datasets in a ternary diagram (Fig. 3). Since the contribution of brGDGTs from either peat or aquatic production could affect the use of brGDGTs for paleoclimate application, in addition to comparing the samples to the global soil dataset (De Jonge et al., 2014), peat and lacustrine sediment samples were added into the ternary plot to help elucidate the provenance of brGDGTs in the BP sediments. According to Sinninghe Damsté (2016), it is imperative to only compare samples in a ternary diagram like this where all of the datasets were analyzed with the novel methods that separate the 5- and 6-methyl brGDGTs since the improved separation can result in an increased quantification of hexamethylated brGDGTs. Recently, samples from East African lake sediments were analyzed using these new methods (Russell et al., 2018) and so these samples were included in the ternary plot for comparison (Fig. 3). Although the lakes from the East African dataset are all from a tropical area, they vary widely in altitude and, thus, in MAAT. We separated them into three categories by MAAT (lakes >20°C, lakes between 10-20°C and lakes<10°C). By comparing all the samples in the ternary plot, it was evident that the BP samples plotted closest to the lacustrine sediment samples from regions in East Africa with a MAAT <10°C, suggesting that the provenance of the majority of the brGDGTs from the BP sediments was not soil or peat but lacustrine aquatic production.

The average estimated surface water pH for the BP sediments (8.6±0.2) calculated using eq. (5), is within the 6 –9 range typical of lakes and rivers (Mattson, 1999). This value is near the upper limit of rich fens characterized by the presence of *S. scorpioides* (Kooijman and Westhoff, 1995; Kooijman and Paulissen, 2006) and is higher than what would be expected for peat-bog sediments that are acidic (pH 3–6; Clymo, 1964) and which constitute most of the peats studied by Naafs et al. (2017). A predominant origin from lake aquatic production is in keeping with previous interpretation of the paleoenvironment of the BP site, which was at least at times covered by water as evidenced by fresh water diatoms, fish remains and gnawed beaver sticks in the sediment (Mitchell et al., 2016).

3.2.2 Aquatic Temperature Transfer Function

Since there is evidence that the majority of the brGDGTs in the BP sediments are aquatically produced, an aquatic transfer function was used for reconstructing temperature. When we apply the African lake calibration (Eq. 4), the

resulting estimated MAAT for BP is 7.1 ± 1.0 °C (mean ± standard deviation). This value is high compared to other previously published estimates from varying proxies, which have estimated MAAT in this region to be in the range of -5.5 to 0.8°C, (Ballantyne et al., 2010; Ballantyne et al., 2006; Csank et al., 2011a; Csank et al., 2011b; Fletcher et al., 2017). A concern when applying this calibration is that it is based on lakes from an equatorial region that does not experience substantial seasonality, whereas, the Pliocene Arctic BP site did experience substantial seasonality (Fletcher et al., 2017). Biological production (including brGDGT production) in BP was likely skewed towards summer and, therefore, summer temperature has a larger influence on the reconstructed MAAT. Unfortunately, no global lake calibration set using individually quantified 5- and 6-methyl brGDGTs is yet available. Therefore, to calculate MST (Eq. 3) we applied the aquatic transfer function developed by Pearson et al. (2011) by combining the individual fractional abundances of the 5- and 6-methyl brGDGTs. The Pearson et al. (2011) calibration was based on a global suite of lake sediments including samples from the Arctic, thus covering a greater range of seasonal variability. The resulting average estimated MST was 15.4 ± 0.8 °C (average ± standard deviation), with temperatures ranging between 14.1 and 17.4 °C (Fig. 4). This is in good agreement with recent estimates based on Climate Reconstruction Analysis using Coexistence Likelihood Estimation (CRACLE; Fletcher et al., 2017) that concluded that MSTs at BP during the Pliocene were approximately 13 to 15°C.

3.3 Vegetation and Fire Reconstruction

All sediment samples from BP contained charcoal (Fig. 4), indicating the consistent prevalence of biomass burning in the High Arctic during this time period. However, counts were variable throughout the section, with the middle and lower sections (mean 34 fragments cm^{-3}) containing less charcoal compared to the upper section upper section (mean 444 fragments cm^{-3}). Overall, samples from BP contained on average 100.0 ± 165 fragments cm^{-3} (mean ± 1 σ), with charcoal area averaging 12.3 ± 20.2 mm^2 cm^{-3}. The variability of charcoal within any given sample was relatively low with a 1 σ among charcoal area of approximately 2 mm^2 cm^{-3}.

The three parts of the section analysed for pollen (380.3–380.4 MASL, 381.15–381.25 MASL, and 381.35–381.45 MASL) reveal variations in vegetation (Figs. 4 and 5). Near the bottom of the section (380.3-380.4 MASL), *Larix* (26%) and *Betula* (17%) were the dominant trees. *Alnus* (6%) and *Salix* (6%) together with ericaceous pollen (4%) were relatively high. In contrast, low numbers of *Picea* (3%), *Pinus* (3%) and fern spores were recorded. Additional wetland taxa like *Myrica* (5%) and Cyperaceae (6%) were also noted. Overall, the non-arboreal (23%) signal was well developed. Crumpled and/or ruptured inaperturate grains with surface sculpturing that varied from scabrate to verricate were noted in the assemblage (12%), but could not be definitely identified. It is possible that these grains represent *Populus*, Cupressaceae or additional Cyperaceae pollen. Between 381.10-381.25 MASL, *Larix* (38%) and *Betula* (21%) increased in abundance, followed by ferns (7%). Cyperaceae remained at similar levels (6%) whereas *Picea* and *Pinus* decreased to 2% and 1%, respectively. Unidentified inaperturate types collectively averaged 14%. *Larix* pollen (23%) remained abundant near the top of the section (381.35-381.45 MASL), whereas *Betula* (2%) decreased. *Picea* (16%) *Pinus* (6%) and ferns (23%) increased in abundance. Of the ferns, trilete spores and cf. *Botrychium* were most abundant, followed by cf. *Dryopteris*. Inaperturate unknowns (10%) were also observed. Other notables included Ericaceae (2%) and Cyperaceae (2%). While rare, Onagraceae grains were also observed (Fig. 5).

According to the GBIF-based mapping exercise, the paleofloral assemblage at BP most closely resembles modern vegetation found in northern North America, particularly on the eastern margin (e.g. New Hampshire, New Brunswick and Nova Scotia) and the western margin (Alaska, Washington, British Columbia, and Alberta; Fig. 7a), and central Fennoscandia. Of these areas, the western coast of northern North America and eastern coast of southern Sweden has the most similarity to the reconstructed BP climate in terms of MST (Fig. 7b) and summer precipitation (Fig. 7c).

While high counts of active fire days are common in the western part of the North American boreal forest, it is not as common in the eastern part of the North American boreal forest (Fig. 7d), likely due to the differences in the precipitation regime. There were also low fire counts in Fennoscandia likely due to historical severe fire suppression (Brown and Giesecke, 2014; Niklasson and Granström, 2004). Therefore, based on our reconstruction of the climate and ecology of the BP site, our results suggest that BP most closely resembled a boreal-type forest ecosystem shaped by fire, similar to those of Washington, British Columbia, Northwest Territories, Yukon and Alaska (but see Sect. 4.3).

4 DISCUSSION

4.1 Geochronology

The plant and animal fossil assemblages observed at BP suggest a depositional age between 3 and 5 Ma (Matthews Jr and Ovenden, 1990; Tedford and Harington, 2003). This biostratigraphic age was corroborated with an amino-acid racemization age (>2.4 ± 0.5 Ma) and Sr-correlation age (2.8–5.1 Ma) on shells (Brigham-Grette and Carter, 1992) in biostratigraphically correlated sediments on Meighen Island, situated 375 km to the west-north-west. The previously calculated burial age of 3.4 Ma for the BP site is a minimum age because no post-depositional production of ^{26}Al or ^{10}Be by muons was assumed. If the samples are considered to have been buried at only the current depth (ca. 10 m, see supplemental data) then the ages plot to the left and outside of the burial field, indicating that the burial depth was significantly deeper for most of the post-depositional history. The revised cosmogenic nuclide burial age is 3.9 +1.5/-0.5 Ma. It is the best interpretation of burial age data based on improved production rate systematics (e.g. Lifton et al., 2014), and more reasonable estimates of erosion rate and ice cover since the mid-Pliocene (see Fig. S3; Table S5). As the stratigraphic position of the cosmogenic samples is very close to the BP peat layers, we interpret the age to represent the approximate time that the peat was deposited.

4.2 Fire, vegetation, temperature: a feedback triangle

Wildfire is a key driver of ecological processes in modern boreal forests (Flannigan et al., 2009; Ryan, 2002), and although historically rare, is becoming more frequent in the tundra in recent years (Mack et al., 2011). The modern increase in fire frequency is likely as a consequence of atmospheric CO_2 driven climate warming and feedbacks such as reduced sea ice extent (Hu et al., 2010), because the probability of fire is highest where temperature and moisture are conducive to growth and drying of fuels followed by conditions that favor ignition (Whitman et al., 2015). Young et al. (2017) confirmed the importance of summer warmth and moisture availability patterns in predicting fire across Alaska, highlighting a July temperature of ~13.5 °C as a key threshold for fire across Alaska.

The abundance of charcoal at BP demonstrates that climatic conditions were conducive to ignition and that sufficient biomass available for combustion existed across the landscape. brGDGTs-derived temperature estimates suggest mean summer temperatures at BP exceeded the ~13.5 °C threshold (Young et al., 2017) that drastically increases the chance of wildfire. Indeed, the estimate of ~15.4°C suggests summer temperatures is ~11°C higher than modern day Eureka, Canada (~4.1°C; Fig. 2). Given a global mean increase of 3°C for the Pliocene compared to modern (see fig. 1) this 11°C increase represents 3.6x arctic amplification of temperature (NB. although comparing summer temperatures to mean global temperature increase is likely imprecise, given much increase of arctic warmth in Pliocene climate models is from winter warming (see Ballantyne at al. 2013) 3.6x is likely an underestimate rather than an overestimate.) Without increasing arctic amplification of temperature that accompanies increasing CO_2, mean summer temperatures would fall below the ~13.5°C threshold. This is evidence that Pliocene arctic amplification of temperatures was a direct feedback to increased wildfire activity, but also an indirect feedback as the increased extent of boreal forest into the higher latitudes, also possible due to arctic amplification of temperatures, provided the fuel (Fig. 6)

An increase in atmospheric convection has been simulated in response to diminished sea-ice during warmer intervals (Abbot and Tziperman, 2008), but this study did not confirm if this increase in atmospheric convection was sufficient to cause lightning ignitions. An alternative ignition source for combustion of biomass on Ellesmere Island during the Pliocene is coal seam fires, which have been documented to be burning at this time (Estrada et al., 2009). However, given the interaction of summer warmth and ignition by lightning within the same climate range as posited for BP, we consider lightning the most likely source of ignition for Pliocene fires in the High Arctic.

Fire return intervals cannot be calculated from the BP charcoal counts due to the absence of a satisfactory age-depth model and discontinuous sampling. As strong interactions are observed between fire regime and ecosystem assemblage in the boreal forest (Brown and Giesecke, 2014; Kasischke and Turetsky, 2006), and in response to climate, comparison with modern fire regimes for areas with shared species compositions and climates may inform a potential range of mean fire return interval (MFRI).

Matthews and Fyles (2000) indicated that the Pliocene BP environment was characterized by an open larch dominated forest-tundra environment, sharing most species in common with those now found in three regions, including central Alaska to Washington in western North America, the region centered around the Canadian/US border in eastern North America, as well as Fennoscandia in Europe. The modern area with the most species in common with BP is central northern Alaska (Fig. 7A). The area over which shared species were calculated is largely tundra, but includes the ecotone between tundra and boreal forest. Other zones that share many species with BP are continuous with Alaska down the western coast of North America to the region around the border of Canada and the United States, the eastern coast of North America in the region around the border of Canada and the United States (~50°N), and central Fennoscandia. Of these zones, the MST of Alaskan tundra sites (6–9°C) are less similar to BP (15.4°C) than ~50°N on both western and eastern coastal North American sites and central Fennoscandia (12–18°C, Fig. 7B). The eastern coast of North America has higher rainfall during the summer (>270 mm), than the west coast and Alaska (Fig. 7C), which correlates to the timing of western fires. The low summer precipitation for much of the west (<200 mm), is consistent with previously published summer precipitation estimates for BP (~190 mm). As a result, the fire regime of the west coast ~50°N may be a better analogue for BP than the east coast of North America. In central

Fennoscandia there is also a west vs. east coastal variation in summer precipitation with the western, Nordic part of the region experiencing higher summer precipitation (252– >288 mm), than the more similar eastern, Swedish part of the region (~198 mm).

Investigation of the modern fire detection data (Fig. 7D) suggests that the two regions most climatically similar to BP, ~50°N western North America and central Sweden, have radically different fire regimes. It is likely this is caused by historical fire suppression in Sweden that limits the utility of modern data for comparison with this study (Brown and Giesecke, 2014; Niklasson and Granström, 2004). To understand the fire regimes, as shaped by climate and species composition rather than human impacts, we considered both the modern and recent Holocene reconstructions for these regions (Table 1). This shows that, a) within any region variation arises from the complex spatial patterning of fire across landscapes, and b) that the regions most similar to BP (~50°N western North American and eastern Fennoscandian reconstructions for the recent Holocene) have shorter fire return intervals than the cooler Alaskan tundra or wetter summer ~50°N region of the eastern North American coast.

While the shared species for Siberia appears low, the number of observations in the modern biodiversity database used is likewise low – perhaps causatively so. Given the similar climate to BP on the Central Siberian Plateau and some key aspects of the floras in Siberia such as the dominance of larch, we considered the fire regime of the larch forests of Siberia. Kharuk et al. (2016; 2011) studied MFRIs across Siberia, from 64°N to 71°N, the northern limit of larch stands. They found an average MFRI across that range of 110 years, with MFRI increasing from 80 years in the southern latitudes to ~300 in the north (Table 1). Based on similarity of the climate variables, the more southerly MFRIs (~80 years) may be a better analogue. Key differences between boreal fires in North America compared to Russia are a higher fire frequency with more burned area in Russia, but a much lower crown fire and a difference in timing of disturbance, with spring fires prevailing in Russia compared to mid-summer fires in western Canada (de Groot et al., 2013; Rogers et al., 2015).

The pollen-based vegetation reconstruction derived in this study indicates that open *Larix-Betula* parkland persisted in the basal (380.3-380.4 MASL) parts of the sequence. Groundcover was additionally dominated by shrub birch, ericaceous heath and ferns. While the regional climate may have been somewhat dry, the record suggests that, locally, a moist fen environment dominated by Cyperaceae, existed near the sampling location. Shrubs including *Alnus* and *Salix* likely occupied the wetland margins.

The corresponding relatively low concentration of charcoal may reflect lower severity fires or higher sedimentation rates. We consider the former more likely due to the depositional environment of Unit III from Mitchell et al. 2016, a lake edge fen peat in a beaver pond or small lake, without evidence of high sediment influx overwhelming peat production. We posit that a surface fire regime, somewhat like that in southern central Siberia existed. This premise is also supported by the fire ecology characteristics of the dominant vegetation. *Larix* does not support crown fires due to leaf moisture content (de Groot et al., 2013) and self-pruning (Kobayashi et al., 2007). The persistence and success of larch in modern-day Siberia appears to be driven by its high growth rate (Jacquelyn et al., 2017) tolerance of frequent surface fire due to thick lower bark (Kobayashi et al., 2007) and tolerance of spring drought due to its deciduous habit (Berg and Chapin III, 1994). Arboreal *Betula* are very intolerant of fire and easily girdled. However, they are quick to resprout and are often found in areas with short fire return intervals. Like *Larix*, arboreal *Betula* have

high moisture content of their foliage and are not prone to crown fires. *Betula* nana L., an extant dwarf birch, is a fire endurer that resprouts from underground rhizomes or roots (Racine et al., 1987) thus regenerating quickly following lower severity fires (de Groot et al., 1997). The vegetation and fire regime characteristics are similar further up the sequence at 381.10-381.25 MASL, with the exception that ferns increased in abundance while heath decreased.

In the upper part of the sequence (381.35-381.45 MASL), where charcoal was abundant, the *Larix-Betula* parkland was replaced by a mixed boreal forest assemblage with a fern understory. Canopy cover was more closed compared to the preceding intervals. The forest was dominated by *Larix* and *Picea*, with lesser amounts of *Pinus*. While *Betula* remained part of the forest, it decreased in abundance possibly due to increased competition with the conifers. Based on exploratory CRACLE analyses of climate preferences using GBIF occurrence data (GBIF.org, 2018a, b, c, d) of the dominant taxa (*Larix-Betula* vs. *Larix-Picea-Pinus*), the expansion of conifers could indicate slightly warmer summers (MST ~15.8 ºC vs. 17.1 ºC). This result differs from the stable MST estimated by bacterial tetraethers, although within reported error, and the small change is certainly within the climate distributions of both communities. The CRACLE analyses also suggest that slightly drier conditions may have prevailed during the three wettest months (249-285mm vs. 192-219mm). While the interaction between climate, vegetation and fire is complex, small changes in MST and precipitation could have directly altered both the vegetation and fire regime, which in turn further promoted fire adapted taxa. In addition to regional climatic factors, community change at the site may have been further influenced by local hydrological conditions, such as channel migration, pond infilling and ecosystem engineering by beaver (*Cantor spp.*).

The high charcoal content of the upper portion (~ Unit IV) of the sequence has three potential explanations: reworking of previously deposited charcoal, decreased sedimentation, or increased wildfire production of charcoal. We consider the first unlikely because there is no difference in the shape of the macrocharcoal between the upper and lower portions of the sequence, whereas we would anticipate a change in the dimensions of the charcoal if it had undergone additional physical breakdown from reworking (see Fig. S4). The second, decreased sedimentation, may occur if the deposition is a result of infrequent, episodic flooding intermixed with long periods during which charcoal was deposited. The recorded sedimentology does not support this explanation, but due to the complexity of flooding processes, also does not disprove this explanation. We, however, favour the third explanation of increased wildfire due to the change in plant composition consistent with a greater influence of fire. If accepted, it is likely that frequent, mixed severity fires persisted. While *Larix* is associated with surface fire, *Picea* and *Pinus* are adapted to higher intensity crown fires. A crown fire regime may have established as conifers expanded, altering fuel loads and flammability. For example, black spruce sheds highly flammable needles, its lower branches can act as fuel ladders facilitating crown fires (Kasischke et al., 2008), and it was previously tentatively identified at BP (Fletcher et al., 2017). While it has thin bark and shallow roots maladapted to survive fire (Auclair, 1985; Brown, 2008; Kasischke et al., 2008), it releases large numbers of seeds from semi-serotinous cones, leading to rapid re-establishment (Côté et al., 2003). The documentation of Onagraceae pollen at the top of the sequence could potentially reflect post-fire succession. For example, the species *Epilobium angustifolium* L. is an early-seral colonizer of disturbed (i.e. burned) sites, pollinated by insects.

It appears that the *Larix-Betula* parkland dominated intervals correspond to the peat- and sand-stratigraphic Units II and III described by Mitchell et al. (2016), whereas the mixed boreal forest in the upper part of the sequence is contemporaneous with Unit IV, described as peat and peaty sand, coarsening upwards. While it is clear that the vegetation and fire regimes changed through time at this Arctic site, temperatures appear more stable, or at least to have no apparent trend. Thus, it is suggested that the fire regime at BP was primarily regulated by regional climate and vegetation, and perhaps additionally by changing local hydrological conditions. Regarding climate, MST remained high enough (> ~13.5ºC) throughout the sequence to allow for fire disturbance and the pollen suggests that temperatures may have marginally increased in the upper part of the sequence. Alternatively, other climate variables, such as the precipitation regime, or local hydrological change may have initiated the change in community. Up-sequence changes in vegetation undoubtedly influenced fine fuel loads and flammability. Indeed, the fire ecological characteristics of the vegetation are consistent with a regional surface fire regime yielding to a crown fire regime.

Betula and *Alnus*, which occurred earlier in the depositional sequence, are favored by beaver in foraging (Busher, 1996; Haarberg and Rosell, 2006; Jenkins, 1979). Moreover, the presence of sticks cut by beaver in Unit III reveals that beavers were indeed at the site, moistening the local land surface. The lack of beaver cut sticks and changes in sediment in Unit IV may indicate that the beavers abandoned the site, possibly in response to changes in vegetation (i.e. increased conifers and decreased *Betula*) limiting preferred forage or due to lateral channel migration, as evidenced by the coarsening upward sequence described by Mitchell et al. (2016). As a result, the local land surface may have become somewhat drier, contemporaneous with the change towards *Larix-Picea-Pinus* forest and a mixed severity fire regime.

Critically, the charcoal record at BP suggests substantial biomass burning that could have acted as a feedback mechanism amplifying or dampening warming during the Pliocene. Its potential role as a feedback to climate is suggested by its prevalence through time, and forest fire's complex direct impacts on the surface radiative budget (e.g. black carbon deposition on snow and ice) and direct and indirect effects on the top of the atmosphere radiative budget (i.e. aerosol emissions; Feng et al., 2016). Further investigation through both investigation of the fire record at other Arctic sites and modelling experiments using varying fire regimes and extent is warranted to better characterize the fire regime in order to improve accuracy of fire simulations in earth system models of Pliocene climate.

5. CONCLUSION

The novel temperature estimates presented here confirm that summer temperatures were considerably warmer during the Pliocene (15.4 ± 0.8 °C) compared to the modern Arctic. The ~11°C higher summer temperatures at Beaver Pond support an increasing influence of arctic amplification of temperatures when CO_2 reaches and exceeds modern levels. Our reconstruction of the paleovegetation and ecology of this unique site on Ellesmere Island suggests an assemblage similar to forests of the western margins of North America and eastern Fennoscandia. The evidence of recurrent fire and concurrent changes in taxonomic composition are indicators that fire played an active role as a feedback in Pliocene Arctic forests, shaping the environment as it does in the boreal forest today. Evidence from fire in the modern boreal forest suggests that fire may have had direct and indirect impacts on Earth's radiative budget at high latitudes during the Pliocene, acting as a feedback to Pliocene climate. The net impact of the component process remains

unknown and modelling experiments are needed to quantitatively investigate the effects of the kind of fire regime presented here, on the Pliocene High Arctic. Collectively, these reconstructions provide new insights into the paleoclimatology and paleoecology of the Canadian High Arctic, ~3.9 Ma.

Data Availability. The data generated and used in this analysis are available in the supplemental information associated with this article.

Sample Availability. Samples used in this analysis are curated by the Canadian Museum of Nature. Sample numbers used for each analysis are given in the supplemental information (Table S3 and S4).

Supplemental Link. To be provided by Copernicus Publishing

Author Contribution. Conceptualization: A.P.B. with modification by other authors; Methodology: J.G., J.S.S.D., K.J.B., T.F.; Formal analysis: All authors; Investigation: A.P.B., J.G., K.J.B., L.W., T.F.; Resources: A.P.B., J.G., J.S.S.D., K.J.B.; Data curation: A.P.B., J.G., K.J.B., L.W., T.F.; Writing—Original draft: All authors; Writing—Review and editing: All authors; Supervision: A.P.B., J.S.S.D., K.J.B., N.R.; Project administration: A.P.B., N.R., T.F.; Funding acquisition: A.P.B., J.G., J.S.S.D., K.J.B., N.R., T.F. (Definitions as per the CRediT Taxonomy)

Competing interests. The authors declare that they have no conflict of interest

Acknowledgements. This work was funded by NSF Polar Programs to A.P.B.; National Geographic Committee for Research and Exploration Grant (9912-16) and Endeavour Research Fellowship (5928-2017) to T.F.; National Geographic Explorer Grant (7902-05), NSERC Discovery Grant (312193), and The W. Garfield Weston Foundation grant to N.R.; student travel (N.R. supervised) was supported by the Northern Scientific Training Program (NSTP) from the government of Canada; an NSERC Discovery Grant (239961) with Northern Supplement (362148) to J.C.G; Natural Resources Canada (SO-03 PA 3.1 Forest Disturbances Wildland Fire) to K.J.B.; the European Research Council under the European Union′s Seventh Framework Programme (FP7/2007-2013) / ERC grant agreement n ° [226600], and funding from the Netherlands Earth System Science Center (NESSC) through a gravitation grant (NWO 024.002.001) from the Dutch Ministry for Education, Culture and Science to J.S.S.D.

. We are also grateful to Nicholas Conder (Canadian Forest Service) who assisted with sample preparation for the vegetation/fire reconstruction. We also acknowledge the 2006, 2008, 2010 and 2012 field teams including D. Finney (Environment Canada), H. Larson (McGill University), M. Vavrek (McGill University), A. Dececchi (McGill University), W.T. Mitchell (Carleton University), R. Smith (University of Saskatchewan), and C. Schröder-Adams (Carleton University). The field research was supported by a paleontology permit from the Government of Nunavut, CLEY (D.R. Stenton, J. Ross) and with the permission of Qikiqtani Inuit Association, especially Grise Fiord (Nunavut). Logistic support was provided by the Polar Continental Shelf Program (M. Bergmann, B. Hyrcyk, B. Hough, M. Kristjanson, T. McConaghy, J. MacGregor and the PCSP team).

References

Abbot, D. S. and Tziperman, E.: Sea ice, high-latitude convection, and equable climates, Geophysical Research Letters, 35, 2008.

Auclair, A. N.: Postfire regeneration of plant and soil organic pools in a *Picea mariana–Cladonia stellaris* ecosystem, Canadian Journal of Forest Research, 15, 279–291, 1985.

Ballantyne, A. P., Axford, Y., Miller, G. H., Otto-Bliesner, B. L., Rosenbloom, N., and White, J. W.: The amplification of Arctic terrestrial surface temperatures by reduced sea-ice extent during the Pliocene, Palaeogeography, Palaeoclimatology, Palaeoecology, 386, 59–67, 2013.

Ballantyne, A. P., Greenwood, D. R., Sinninghe Damsté, J. S., Csank, A. Z., Eberle, J. J., and Rybczynski, N.: Significantly warmer Arctic surface temperatures during the Pliocene indicated by multiple independent proxies, Geology, 38, 603–606, 2010.

Ballantyne, A. P., Rybczynski, N., Baker, P. A., Harington, C. R., and White, D.: Pliocene Arctic temperature constraints from the growth rings and isotopic composition of fossil larch, Palaeogeography, Palaeoclimatology, Palaeoecology, 242, 188–200, 2006.

Bendle, J. A., Weijers, J. W., Maslin, M. A., Sinninghe Damsté, J. S., Schouten, S., Hopmans, E. C., Boot, C. S., and Pancost, R. D.: Major changes in glacial and Holocene terrestrial temperatures and sources of organic carbon recorded in the Amazon fan by tetraether lipids, Geochemistry, Geophysics, Geosystems, 11, 2010.

Berg, E. E. and Chapin III, F. S.: Needle loss as a mechanism of winter drought avoidance in boreal conifers, Canadian Journal of Forest Research, 24, 1144–1148, 1994.

Bergeron, Y.: The influence of island and mainland lakeshore landscapes on boreal forest fire regimes, Ecology, 72, 1980–1992, 1991.

Bergeron, Y., Cyr, D., Drever, C. R., Flannigan, M., Gauthier, S., Kneeshaw, D., Lauzon, È., Leduc, A., Goff, H. L., Lesieur, D., and Logan, K.: Past, current, and future fire frequencies in Quebec's commercial forests: implications for the cumulative effects of harvesting and fire on age-class structure and natural disturbance-based management, Canadian Journal of Forest Research, 36, 2737–2744, 2006.

Bouchard, M., Pothier, D., and Gauthier, S.: Fire return intervals and tree species succession in the North Shore region of eastern Quebec, Canadian Journal of Forest Research, 38, 1621–1633, 2008.

Brigham-Grette, J. and Carter, L. D.: Pliocene Marine Transgressions of Northern Alaska: Circumarctic Correlations and Paleoclimatic Interpretations, Arctic, 45, 74–89, 1992.

Brown, K. J. and Giesecke, T.: Holocene fire disturbance in the boreal forest of central Sweden, Boreas, 43, 639–651, 2014.

Brown, K. J. and Power, M. J.: Charred particle analyses. In: Encyclopedia of Quaternary Science, Elias, S. (Ed.), Elsevier, Amsterdam, 2013.

Brown, M.: Fire and Ice: Fire Severity and Future Flammability in Alaskan Black Spruce Forests, Fire Science Brief, 2008. 1–6, 2008.

Bush, E. and Lemmen, D.S.(eds): Canada's Changing Climate Report; Government of Canada, Ottawa, ON. 444 p., 2019

Busher, P. E.: Food Caching Behavior of Beavers (*Castor canadensis*): Selection and Use of Woody Species, The American Midland Naturalist, 135, 343-348, 1996.

Clymo, R. S.: The Origin of Acidity in Sphagnum Bogs, The Bryologist, 67, 427–431, 1964.

Côté, M., Ferron, J., and Gagnon, R.: Impact of seed and seedling predation by small rodents on early regeneration establishment of black spruce, Canadian Journal of Forest Research, 33, 2362–2371, 2003.

Csank, A. Z., Patterson, W. P., Eglington, B. M., Rybczynski, N., and Basinger, J. F.: Climate variability in the Early Pliocene Arctic: Annually resolved evidence from stable isotope values of sub-fossil wood, Ellesmere Island, Canada, Palaeogeography, Palaeoclimatology, Palaeoecology, 308, 339–349, 2011a.

Csank, A. Z., Tripati, A. K., Patterson, W. P., Eagle, R. A., Rybczynski, N., Ballantyne, A. P., and Eiler, J. M.: Estimates of Arctic land surface temperatures during the early Pliocene from two novel proxies, Earth and Planetary Science Letters, 304, 291–299, 2011b.

de Groot, W. J., Cantin, A. S., Flannigan, M. D., Soja, A. J., Gowman, L. M., and Newbery, A.: A comparison of Canadian and Russian boreal forest fire regimes, Forest Ecology and Management, 294, 23–34, 2013.

de Groot, W. J., Thomas, P. A., and Wein, R. W.: *Betula nana* L. *and Betula glandulosa* Michx, Journal of Ecology, 85, 241–264, 1997.

De Jonge, C., Hopmans, E. C., Stadnitskaia, A., Rijpstra, W. I. C., Hofland, R., Tegelaar, E., and Sinninghe Damsté, J. S.: Identification of novel penta-and hexamethylated branched glycerol dialkyl glycerol tetraethers in peat using HPLC–MS 2, GC–MS and GC–SMB-MS, Organic geochemistry, 54, 78–82, 2013.

De Jonge, C., Hopmans, E. C., Zell, C. I., Kim, J.-H., Schouten, S., and Sinninghe Damsté, J. S.: Occurrence and abundance of 6-methyl branched glycerol dialkyl glycerol tetraethers in soils: Implications for palaeoclimate reconstruction, Geochimica et Cosmochimica Acta, 141, 97–112, 2014.

De Jonge, C., Stadnitskaia, A., Hopmans, E. C., Cherkashov, G., Fedotov, A., Streletskaya, I. D., Vasiliev, A. A., and Sinninghe Damsté, J. S.: Drastic changes in the distribution of branched tetraether lipids in suspended matter and sediments from the Yenisei River and Kara Sea (Siberia): Implications for the use of brGDGT-based proxies in coastal marine sediments, Geochimica et Cosmochimica Acta, 165, 200–225, 2015.

de Lafontaine, G. and Payette, S.: Shifting zonal patterns of the southern boreal forest in eastern Canada associated with changing fire regime during the Holocene, Quaternary Science Reviews, 30, 867–875, 2011.

Dowsett, H., Dolan, A., Rowley, D., Pound, M., Salzmann, U., Robinson, M., Chandler, M., Foley, K., and Haywood, A.: The PRISM4 (mid-Piacenzian) palaeoenvironmental reconstruction, Climate of the Past, doi: doi:10.5194/cp-12-1519-2016, 2016. 2016.

Dowsett, H. J., Cronin, T. M., Poore, R. Z., Thompson, R. S., Whatley, R. C., and Wood, A. M.: Micropaleontological evidence for increased meridional heat transport in the North Atlantic Ocean during the Pliocene, Science, 258, 1133–1136, 1992.

Dowsett, H. J., Robinson, M. M., Haywood, A. M., Hill, D. J., Dolan, A. M., Stoll, D. K., Chan, W. L., Abe-Ouchi, A., Chandler, M. A., and Rosenbloom, N. A.: Assessing confidence in Pliocene sea surface temperatures to evaluate predictive models, Nature Climate Change, 2, 365–371, 2012.

576 Estrada, S., Piepjohn, K., Frey, M. J., Reinhardt, L., Andruleit, H., and von Gosen, W.: Pliocene coal-seam fires on
577 southern Ellesmere Island, Canadian Arctic, Neues Jahrbuch für Geologie und Paläontologie - Abhandlungen, 251,
578 33-52, 2009.
579 Feng, R., Otto-Bliesner, B., Fletcher, T., Ballantyne, A., and Brady, E.: Contributions to Pliocene Arctic warmth from
580 removal of anthropogenic aerosol and enhanced forest fire emissions, San Francisco, USA. 2016, PP33A-2344.
581 Feng, R., Otto-Bliesner, B. L., Fletcher, T. L., Tabor, C. R., Ballantyne, A. P., and Brady, E. C.: Amplified Late
582 Pliocene terrestrial warmth in northern high latitudes from greater radiative forcing and closed Arctic Ocean gateways,
583 Earth and Planetary Science Letters, 466, 129-138, 2017.
584 Flannigan, M., Stocks, B., Turetsky, M., and Wotton, M.: Impacts of climate change on fire activity and fire
585 management in the circumboreal forest, Global Change Biology, 15, 549–560, 2009.
586 Fletcher, T., Feng, R., Telka, A. M., Matthews, J. V., and Ballantyne, A.: Floral dissimilarity and the influence of
587 climate in the Pliocene High Arctic: Biotic and abiotic influences on five sites on the Canadian Arctic Archipelago,
588 Frontiers in Ecology and Evolution, 5, 19, 2017.
589 Foster, L. C., Pearson, E. J., Juggins, S., Hodgson, D. A., Saunders, K. M., Verleyen, E., and Roberts, S. J.:
590 Development of a regional glycerol dialkyl glycerol tetraether (GDGT)–temperature calibration for Antarctic and sub-
591 Antarctic lakes, Earth and Planetary Science Letters, 433, 370–379, 2016.
592 Francis, J. and Skific, N.: Evidence linking rapid Arctic warming to mid-latitude weather patterns, Philosophical
593 Transactions of the Royal Society A: Mathematical, Physical and Engineering Sciences, 373, 1–12, 2015.
594 GBIF.org: GBIF Occurrence Download (Beaver Pond extant species) http://doi.org/10.15468/dl.ertiqj 1st February
595 2017.
596 GBIF.org: GBIF Occurrence Download (*Betula*) https://doi.org/10.15468/dl.akxgp5 11th May 2018a.
597 GBIF.org: GBIF Occurrence Download (*Larix*) https://doi.org/10.15468/dl.mfhnci 11th May 2018b.
598 GBIF.org: GBIF Occurrence Download (*Picea*) https://doi.org/10.15468/dl.wi7jdc 11th May 2018c.
599 GBIF.org: GBIF Occurrence Download (*Pinus*) https://doi.org/10.15468/dl.vwfjj2 11th May 2018d.
600 Greene, G. A. and Daniels, L. D.: Spatial interpolation and mean fire interval analyses quantify historical mixed-
601 severity fire regimes, International Journal of Wildland Fire, 26, 136–147, 2017.
602 Haarberg, O. and Rosell, F.: Selective foraging on woody plant species by the Eurasian beaver (*Castor fiber*) in
603 Telemark, Norway, Journal of Zoology, 270, 201-208, 2006.
604 Haywood, A. M., Dowsett, H. J., and Dolan, A. M.: Integrating geological archives and climate models for the mid-
605 Pliocene warm period, Nature communications, 7, 1-14, 2016.
606 Higuera, P., Barnes, J. L., Chipman, M. L., Urban, M., and Hu, F. S.: The burning tundra: A look back at the last 6,000
607 years of fire in the Noatak National Preserve, Northwestern Alaska, Alaska Park Science, 10, 37–41, 2011.
608 Higuera, P. E., Brubaker, L. B., Anderson, P. M., Hu, F. S., and Brown, T. A.: Vegetation mediated the impacts of
609 postglacial climate change on fire regimes in the south-central Brooks Range, Alaska, Ecological Monographs, 79,
610 201–219, 2009.
611 Hijmans, R. J., Cameron, S. E., Parra, J. L., Jones, P. G., and Jarvis, A.: Very high resolution interpolated climate
612 surfaces for global land areas, International Journal of Climatology, 25, 1965–1978, 2005.

Hopmans, E. C., Schouten, S., and Sinninghe Damsté, J. S.: The effect of improved chromatography on GDGT-based palaeoproxies, Organic Geochemistry, 93, 1–6, 2016.

Hu, F. S., Higuera, P. E., Walsh, J. E., Chapman, W. L., Duffy, P. A., Brubaker, L. B., and Chipman, M. L.: Tundra burning in Alaska: Linkages to climatic change and sea ice retreat, Journal of Geophysical Research: Biogeosciences, 115, 2010.

Huguet, C., Hopmans, E. C., Febo-Ayala, W., Thompson, D. H., Sinninghe Damsté, J. S., and Schouten, S.: An improved method to determine the absolute abundance of glycerol dibiphytanyl glycerol tetraether lipids, Organic Geochemistry, 37, 1036–1041, 2006.

Hwang, Y. T., Frierson, D. M., and Kay, J. E.: Coupling between Arctic feedbacks and changes in poleward energy transport, Geophysical Research Letters, 38, 2011.

Jacquelyn, K. S., Adrianna, C. F., Herman, H. S., Amanda, H.-H., Alexander, K., Tatiana, L., Dmitry, E., and Elena, S.: Fire disturbance and climate change: implications for Russian forests, Environmental Research Letters, 12, 035003, 2017.

Jenkins, S. H.: Seasonal and year-to-year differences in food selection by beavers, Oecologia, 44, 112-116, 1979.

Johnstone, J. F., Chapin, F. S., Hollingsworth, T. N., Mack, M. C., Romanovsky, V., and Turetsky, M.: Fire, climate change, and forest resilience in interior Alaska, Canadian Journal of Forest Research, 40, 1302–1312, 2010a.

Johnstone, J. F., Hollingsworth, T. N., Chapin, F. S., and Mack, M. C.: Changes in fire regime break the legacy lock on successional trajectories in Alaskan boreal forest, Global Change Biology, 16, 1281–1295, 2010b.

Johnstone, J. F. and Kasischke, E. S.: Stand-level effects of soil burn severity on postfire regeneration in a recently burned black spruce forest, Canadian Journal of Forest Research, 35, 2151–2163, 2005.

Jones, P. D. and Moberg, A.: Hemispheric and large-scale surface air temperature variations: An extensive revision and an update to 2001, Journal of Climate, 16, 206–223, 2003.

Kasischke, E. S. and Turetsky, M. R.: Recent changes in the fire regime across the North American boreal region—spatial and temporal patterns of burning across Canada and Alaska, Geophysical research letters, 33, 2006.

Kasischke, E. S., Turetsky, M. R., Ottmar, R. D., French, N. H., Hoy, E. E., and Kane, E. S.: Evaluation of the composite burn index for assessing fire severity in Alaskan black spruce forests, International Journal of Wildland Fire, 17, 515–526, 2008.

Kasischke, E. S., Williams, D., and Barry, D.: Analysis of the patterns of large fires in the boreal forest region of Alaska, International Journal of Wildland Fire, 11, 131–144, 2002.

Kharuk, V. I., Dvinskaya, M. L., Petrov, I. A., Im, S. T., and Ranson, K. J.: Larch forests of Middle Siberia: long-term trends in fire return intervals, Regional Environmental Change, doi: 10.1007/s10113-016-0964-9, 2016. 1–9, 2016.

Kharuk, V. I., Ranson, K. J., Dvinskaya, M. L., and Im, S. T.: Wildfires in northern Siberian larch dominated communities, Environmental Research Letters, 6, 045208, 2011.

Kobayashi, M., Nemilostiv, Y. P., Zyryanova, O. A., Kajimoto, T., Matsuura, Y., Yoshida, T., Satoh, F., Sasa, K., and Koike, T.: Regeneration after forest fires in mixed conifer broad-leaved forests of the Amur region in far eastern Russia: the relationship between species specific traits against fire and recent fire regimes, Eurasian Journal of Forest Research, 10, 51–58, 2007.

650 Kooijman, A. and Westhoff, V.: Variation in habitat factors and species composition of *Scorpidium scorpioides*
651 communities in NW-Europe, Plant Ecology, 117, 133–150, 1995.
652 Kooijman, A. M. and Paulissen, M. P. C. P.: Higher acidification rates in fens with phosphorus enrichment, Applied
653 Vegetation Science, 9, 205–212, 2006.
654 Lifton, N., Sato, T., and Dunai, T. J.: Scaling in situ cosmogenic nuclide production rates using analytical
655 approximations to atmospheric cosmic-ray fluxes, Earth and Planetary Science Letters, 386, 149–160, 2014.
656 Lisiecki, L. E. and Raymo, M. E.: A Plio-Pleistocene stack of 57 globally distributed benthic $\delta^{18}O$ records,
657 Paleoceanography, 20, 2005.
658 Loomis, S. E., Russell, J. M., Ladd, B., Street-Perrott, F. A., and Sinninghe Damsté, J. S.: Calibration and application
659 of the branched GDGT temperature proxy on East African lake sediments, Earth and Planetary Science Letters, 357,
660 277–288, 2012.
661 Lorimer, C. G.: The Presettlement Forest and Natural Disturbance Cycle of Northeastern Maine, Ecology, 58, 139–
662 148, 1977.
663 Luthi, D., Le Floch, M., Bereiter, B., Blunier, T., Barnola, J.-M., Siegenthaler, U., Raynaud, D., Jouzel, J., Fischer,
664 H., Kawamura, K., and Stocker, T. F.: High-resolution carbon dioxide concentration record 650,000-800,000 years
665 before present, Nature, 453, 379–382, 2008.
666 Lynch, J. A., Clark, J. S., Bigelow, N. H., Edwards, M. E., and Finney, B. P.: Geographic and temporal variations in
667 fire history in boreal ecosystems of Alaska, Journal of Geophysical Research: Atmospheres, 107, FFR 8-1–FFR 8-17,
668 2002.
669 Mack, M. C., Bret-Harte, M. S., Hollingsworth, T. N., Jandt, R. R., Schuur, E. A. G., Shaver, G. R., and Verbyla, D.
670 L.: Carbon loss from an unprecedented Arctic tundra wildfire, Nature, 475, 489–492, 2011.
671 Marshall, J., Armour, K. C., Scott, J. R., Kostov, Y., Hausmann, U., Ferreira, D., Shepherd, T. G., and Bitz, C. M.:
672 The ocean's role in polar climate change: asymmetric Arctic and Antarctic responses to greenhouse gas and ozone
673 forcing, Philosophical Transactions of the Royal Society of London A: Mathematical, Physical and Engineering
674 Sciences, 372, 20130040, 2014.
675 Matthews Jr, J. V. and Ovenden, L. E.: Late Tertiary plant macrofossils from localities in Arctic/sub- Arctic North
676 America: a review of the data, Arctic, 43, 364–392, 1990.
677 Matthews, J. V. J. and Fyles, J. G.: Late Tertiary plant and arthropod fossils from the High Terrace Sediments on the
678 Fosheim Peninsula of Ellesmere Island (Northwest Territories, District of Franklin), Geological Survey of Canada,
679 Bulletin, 529, 295–317, 2000.
680 Mattson, M. D.: Acid lakes and rivers. In: Environmental Geology, Springer Netherlands, Dordrecht, 1999.
681 McAndrews, J. H., Berti, A. A., and Norris, G.: Key to the Quaternary pollen and spores of the Great Lakes region,
682 1973. 1973.
683 Miller, G. H., Alley, R. B., Brigham-Grette, J., Fitzpatrick, J. J., Polyak, L., Serreze, M. C., and White, J. W. C.: Arctic
684 amplification: can the past constrain the future?, Quaternary Science Reviews, 29, 1779–1790, 2010.

Mitchell, W. T., Rybczynski, N., Schröder-Adams, C., Hamilton, P. B., Smith, R., and Douglas, M.: Stratigraphic and Paleoenvironmental Reconstruction of a Mid-Pliocene Fossil Site in the High Arctic (Ellesmere Island, Nunavut): Evidence of an Ancient Peatland with Beaver Activity, Arctic, 69, 185–204, 2016.

Moore, P. D., Webb, J. A., and Collison, M. E.: Pollen analysis, Blackwell Scientific Publications, Oxford, 1991.

Naafs, B., Inglis, G., Zheng, Y., Amesbury, M., Biester, H., Bindler, R., Blewett, J., Burrows, M., del Castillo Torres, D., and Chambers, F. M.: Introducing global peat-specific temperature and pH calibrations based on brGDGT bacterial lipids, Geochimica et Cosmochimica Acta, 208, 285–301, 2017.

Niemann, H., Stadtnitskaia, A., Wirth, S., Gilli, A., Anselmetti, F., Sinninghe Damsté, J., Schouten, S., Hopmans, E., and Lehmann, M.: Bacterial GDGTs in Holocene sediments and catchment soils of a high Alpine lake: application of the MBT/CBT-paleothermometer, Climate of the Past, 8, 889-906, 2012.

Niklasson, M. and Drakenberg, B.: A 600-year tree-ring fire history from Norra Kvills National Park, southern Sweden: implications for conservation strategies in the hemiboreal zone, Biological Conservation, 101, 63–71, 2001.

Niklasson, M. and Granström, A.: Fire in Sweden – History, Research, Prescribed Burning and Forest Certification, International Forest Fire News, 30, 80–83, 2004.

Niklasson, M. and Granström, A.: Numbers and sizes of fires: Long-term spatially explicit fire history in a Swedish boreal landscape, Ecology, 81, 1484–1499, 2000.

Otto-Bliesner, B. L. and Upchurch Jr, G. R.: Vegetation-induced warming of high-latitude regions during the Late Cretaceous period, Nature, 385, 804, 1997.

Pagani, M., Liu, Z., LaRiviere, J., and Ravelo, A. C.: High Earth-system climate sensitivity determined from Pliocene carbon dioxide concentrations, Nature Geoscience, 3, 27–30, 2010.

Pearson, E. J., Juggins, S., Talbot, H. M., Weckström, J., Rosén, P., Ryves, D. B., Roberts, S. J., and Schmidt, R.: A lacustrine GDGT-temperature calibration from the Scandinavian Arctic to Antarctic: Renewed potential for the application of GDGT-paleothermometry in lakes, Geochimica et Cosmochimica Acta, 75, 6225–6238, 2011.

Peterse, F., Prins, M. A., Beets, C. J., Troelstra, S. R., Zheng, H., Gu, Z., Schouten, S., and Sinninghe Damsté, J. S.: Decoupled warming and monsoon precipitation in East Asia over the last deglaciation, Earth and Planetary Science Letters, 301, 256–264, 2011.

Powers, L. A., Werne, J. P., Johnson, T. C., Hopmans, E. C., Sinninghe Damsté, J. S., and Schouten, S.: Crenarchaeotal membrane lipids in lake sediments: A new paleotemperature proxy for continental paleoclimate reconstruction?, Geology, 32, 613–616, 2004.

R Core Team: R: A language and environment for statistical computing. R Foundation for Statistical Computing, Vienna, Austria, 2016.

Racine, C. H., Johnson, L. A., and Viereck, L. A.: Patterns of Vegetation Recovery after Tundra Fires in Northwestern Alaska, U.S.A, Arctic and Alpine Research, 19, 461–469, 1987.

Robinson, M. M.: New Quantitative Evidence of Extreme Warmth in the Pliocene Arctic, Stratigraphy, 6, 265–275, 2009.

Rogers, B. M., Soja, A. J., Goulden, M. L., and Randerson, J. T.: Influence of tree species on continental differences in boreal fires and climate feedbacks, Nature Geoscience, 8, 228–234, 2015.

Royer, D. L., Berner, R. A., and Park, J.: Climate sensitivity constrained by CO_2 concentrations over the past 420 million years, Nature, 446, 530-532, 2007.

Russell, J. M., Hopmans, E. C., Loomis, S. E., Liang, J., and Sinninghe Damsté, J. S.: Distributions of 5- and 6-methyl branched glycerol dialkyl glycerol tetraethers (brGDGTs) in East African lake sediment: Effects of temperature, pH, and new lacustrine paleotemperature calibrations, Geochimica et Cosmochimica Acta, 117, 56–69, 2018.

Ryan, K. C.: Dynamic interactions between forest structure and fire behavior in boreal ecosystems, Silva Fennica, 36, 13–39, 2002.

Rybczynski, N., Gosse, J. C., Richard Harington, C., Wogelius, R. A., Hidy, A. J., and Buckley, M.: Mid-Pliocene warm-period deposits in the High Arctic yield insight into camel evolution, Nature Communications, 4, 1–9, 2013.

Salzmann, U., Dolan, A. M., Haywood, A. M., Chan, W.-L., Voss, J., Hill, D. J., Abe-Ouchi, A., Otto-Bliesner, B., Bragg, F. J., and Chandler, M. A.: Challenges in quantifying Pliocene terrestrial warming revealed by data-model discord, Nature Climate Change, 3, 969, 2013.

Salzmann, U., Haywood, A. M., Lunt, D., Valdes, P., and Hill, D.: A new global biome reconstruction and data-model comparison for the middle Pliocene, Global Ecology and Biogeography, 17, 432–447, 2008.

Shellito, C. J., Lamarque, J.-F. o., and Sloan, L. C.: Early Eocene Arctic climate sensitivity to pCO_2 and basin geography, Geophysical Research Letters, 36, 2009.

Sinninghe Damsté, J. S.: Spatial heterogeneity of sources of branched tetraethers in shelf systems: The geochemistry of tetraethers in the Berau River delta (Kalimantan, Indonesia), Geochimica et Cosmochimica Acta, 186, 13–31, 2016.

Sinninghe Damsté J.S., Rijpstra W.I.C., Foesel B.U., Huber K., Overmann J., Nakagawa S., Joong Jae Kim, Dunfield P.F. Dedysh S.N., Villanueva L. (2018) An overview of the occurrence of ether- and ester-linked iso-diabolic acid membrane lipids in microbial cultures of the Acidobacteria: Implications for brGDGT palaeoproxies for temperature and pH. Organic Geochemistry, 124, 63–76.

Sinninghe Damsté, J. S., Rijpstra, W. I. C., Hopmans, E. C., Foesel, B. U., Wüst, P. K., Overmann, J., Tank, M., Bryant, D. A., Dunfield, P. F., Houghton, K., and Stott, M. B.: Ether- and Ester-Bound iso-Diabolic Acid and Other Lipids in Members of Acidobacteria Subdivision 4, Applied and Environmental Microbiology, 80, 5207–5218, 2014.

Sinninghe Damsté, J. S., Rijpstra, W. I. C., Hopmans, E. C., Weijers, J. W., Foesel, B. U., Overmann, J., and Dedysh, S. N.: 13, 16-Dimethyl octacosanedioic acid (iso-diabolic acid), a common membrane-spanning lipid of Acidobacteria subdivisions 1 and 3, Applied and Environmental Microbiology, 77, 4147–4154, 2011.

Stap, L. B., de Boer, B., Ziegler, M., Bintanja, R., Lourens, L. J., and van de Wal, R. S.: CO_2 over the past 5 million years: Continuous simulation and new δ11B-based proxy data, Earth and Planetary Science Letters, 439, 1–10, 2016.

Swann, A. L., Fung, I. Y., Levis, S., Bonan, G. B., and Doney, S. C.: Changes in Arctic vegetation amplify high-latitude warming through the greenhouse effect, Proceedings of the National Academy of Sciences of the United States of America, 107, 1295-1300, 2010.

Tedford, R. H. and Harington, C. R.: An Arctic mammal fauna from the early Pliocene of North America, Nature, 425, 388–390, 2003.

Van Wagner, C. E., Finney, M. A., and Heathcott, M.: Historical fire cycles in the Canadian Rocky Mountain parks, Forest Science, 52, 704-717, 2006.

Wang, X., Rybczynski, N., Harington, C. R., White, S. C., and Tedford, R. H.: A basal ursine bear (*Protarctos abstrusus*) from the Pliocene High Arctic reveals Eurasian affinities and a diet rich in fermentable sugars, Scientific reports, 7, 17722, 2017.

Warden, L., Jung-Hyun, K., Zell, C., Vis, G.-J., de Stigter, H., Bonnin, J., and Sinninghe Damsté, J. S.: Examining the provenance of branched GDGTs in the Tagus River drainage basin and its outflow into the Atlantic Ocean over the Holocene to determine their usefulness for paleoclimate applications, Biogeosciences, 13, 5719, 2016.

Weijers, J. W., Schefuß, E., Schouten, S., and Sinninghe Damsté, J. S.: Coupled thermal and hydrological evolution of tropical Africa over the last deglaciation, Science, 315, 1701–1704, 2007a.

Weijers, J. W., Schouten, S., van den Donker, J. C., Hopmans, E. C., and Sinninghe Damsté, J. S.: Environmental controls on bacterial tetraether membrane lipid distribution in soils, Geochimica et Cosmochimica Acta, 71, 703-713, 2007b.

Weijers, J. W. H., Schouten, S., van den Donker, J. C., Hopmans, E. C., and Sinninghe Damsté, J. S.: Environmental controls on bacterial tetraether membrane lipid distribution in soils, Geochimica et Cosmochimica Acta, 71, 703-713, 2007c.

Whitman, E., Batllori, E., Parisien, M. A., Miller, C., Coop, J. D., Krawchuk, M. A., Chong, G. W., and Haire, S. L.: The climate space of fire regimes in north-western North America, Journal of Biogeography, 42, 1736–1749, 2015.

Wright, C. S. and Agee, J. K.: Fire and vegetation history in the eastern Cascade Mountains, Washington, Ecological Applications, 14, 443–459, 2004.

Yang, G., Zhang, C. L., Xie, S., Chen, Z., Gao, M., Ge, Z., and Yang, Z.: Microbial glycerol dialkyl glycerol tetraethers from river water and soil near the Three Gorges Dam on the Yangtze River, Organic Geochemistry, 56, 40–50, 2013.

Yarie, J.: Forest fire cycles and life tables: a case study from interior Alaska, Canadian Journal of Forest Research, 11, 554–562, 1981.

Young, A. M., Higuera, P. E., Duffy, P. A., and Hu, F. S.: Climatic thresholds shape northern high-latitude fire regimes and imply vulnerability to future climate change, Ecography, 40, 606–617, 2017.

Zech, R., Gao, L., Tarozo, R., and Huang, Y.: Branched glycerol dialkyl glycerol tetraethers in Pleistocene loess-paleosol sequences: three case studies, Organic geochemistry, 53, 38–44, 2012.

Zell, C., Kim, J.-H., Moreira-Turcq, P., Abril, G., Hopmans, E. C., Bonnet, M.-P., Sobrinho, R. L., and Sinninghe Damsté, J. S.: Disentangling the origins of branched tetraether lipids and crenarchaeol in the lower Amazon River: Implications for GDGT-based proxies, Limnology and Oceanography, 58, 343–353, 2013.

Zhu, C., Weijers, J. W., Wagner, T., Pan, J.-M., Chen, J.-F., and Pancost, R. D.: Sources and distributions of tetraether lipids in surface sediments across a large river-dominated continental margin, Organic Geochemistry, 42, 376–386, 2011.

Zink, K.-G., Vandergoes, M. J., Mangelsdorf, K., Dieffenbacher-Krall, A. C., and Schwark, L.: Application of bacterial glycerol dialkyl glycerol tetraethers (GDGTs) to develop modern and past temperature estimates from New Zealand lakes, Organic Geochemistry, 41, 1060–1066, 2010.

795 **Table 1. Modern and recent Holocene fire return interval reconstructions for the candidate analogous regions considered**
796 **in this study.**

Region	Modern		Reference	Recent Holocene		Reference
Alaskan Tundra	Seward Peninsula	273*	Kasischke et al. (2002)	Up-Valley	263	Higuera et al. (2011)
	Nulato Hills	306*		Down-valley	142	
Alaskan Boreal	Porcupine/ Upper Yukon (Central)	~100	Yarie (1981)			
	Sites near Fairbanks, and Delta Junction (Central)	70130	Johnstone et al. (2010a); Johnstone et al. (2010b); Johnstone and Kasischke (2005)			
	Kenai Peninsula		Lynch et al. (2002)	Interior Alaska and Kenai Peninsula	198 ± 90	Lynch et al. (2002)
	Yukon river Lowlands	120	Kasischke et al. (2002)	Brooks Range	145	Higuera et al. (2009)
	Kuskokwim Mountains	218				
	Yukon-Tanama Uplands	330				
	Tanana-Kuskokwim Lowlands	178				
	Kobuk Ridges and Valleys	175				
	Davidson Mountains	403				
	North Ogilive Mountains	112				
	Ray Mountains	109				
	Yukon-Old Crow Basin	81				

Western North America	Darkwoods, British Columbia	~69	Greene and Daniels (2017)			
	Cascade Mountains, Washington	~27	Wright and Agee (2004)			
	Desolation Peak, Washington Coastal type	108-137				
	Desolation Peak, Washington Interior type	~52				
Eastern North America	Quebec – west	~270*	Bouchard et al. (2008)	Maine	≥ 800	Lorimer (1977)
	Quebec – east	>500*				
				Quebec – "Spruce zone"	570	de Lafontaine and Payette (2011)
				Quebec – "Fir zone"	>1000	
	Quebec – Abitibi northwest	418*	Bergeron et al. (2006 post-1940)^	Quebec – Abitibi northwest	189	Bergeron et al. (2006 post-1940)^
	Quebec – Abitibi southwest	388*		Quebec – Abitibi southwest	165	
	Quebec – Abitibi east	418*		Quebec – Abitibi east	141	
	Quebec – Abitibi southeast	2083*		Quebec – Abitibi southeast	257	
	Quebec – Temiscamingue north	2083*		Quebec – Temiscamingue north	220	

	Quebec – Temiscamingue south	2777*		Quebec – Temiscamingue south	313	
	Quebec – Waswanipi	418*		Quebec – Waswanipi	128	
	Quebec – Central Quebec	388*		Quebec – Central Quebec	150	
	Quebec – North Shore	645*		Quebec – North Shore	281	
	Quebec – Gaspésia	488*		Quebec – Gaspésia	161	
	Quebec – northwestern - lakeshore	99’	Bergeron (1991)	Quebec – northwestern - lakeshore	63’	Bergeron (1991)
	Quebec – northwestern – lake island	112’		Quebec – northwestern – lake island	74’	
Fennoscandia	Sweden	*	Niklasson and Drakenberg (2001); Niklasson and Granström (2004)	North Sweden	50-150	Niklasson and Granström (2004); Niklasson and Granström (2000)
				Southern Sweden	20	Niklasson and Drakenberg (2001)
	Central Sweden	*	Brown and Giesecke (2014)	Central Sweden - Klotjärnen	180	Brown and Giesecke (2014)
				Central Sweden - Holtjärnen	240	
Siberian Plateau	Northern	300	Kharuk et al. (2016); Kharuk et al. (2011)			
	Southern	80				
	Mean (64-71°N)	110				

797 ^ = The reciprocal converted from burn rate (%) (see Van Wagner et al., 2006)

798 * = Estimates likely effected in some areas by human activity. In such instances Recent Holocene is preferred.

799 ‘ = Fire cycle

800 †=‘Recent’ here refers to records that (or have distinct sections that) begin after the end of the Holocene Climate

801 Optima and end near present

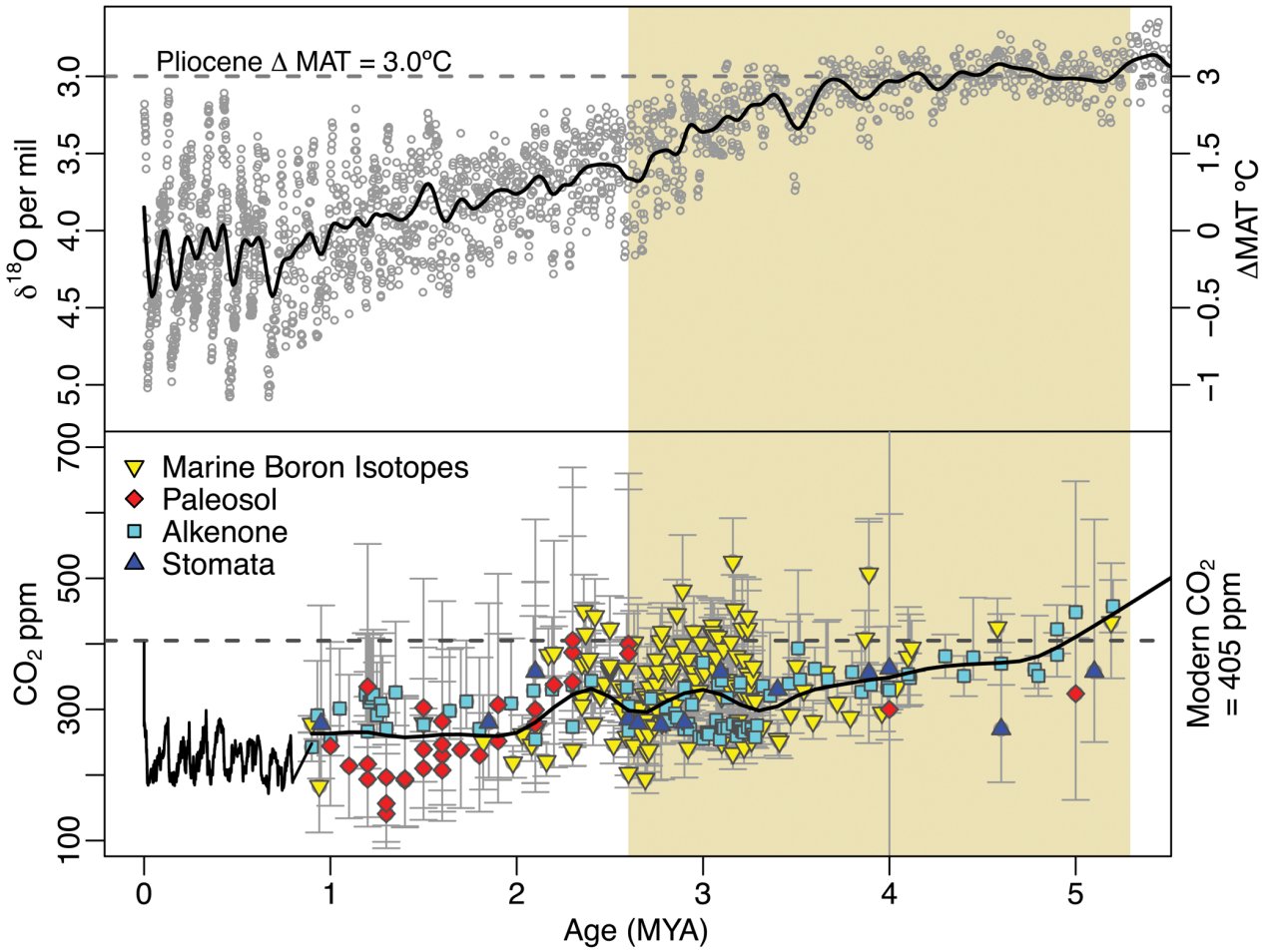

Figure 1: Global temperatures and atmospheric CO_2 concentration spanning the last 5 million years of Earth's history. Mean annual temperatures (MAT) are inferred from compiled $\delta^{18}O$ foraminifera data (Lisiecki and Raymo, 2005) and plotted as anomalies from present (top panel). Modern atmospheric CO_2 measurements (NOAA/ESRL), and ice core observations from EPICA (Luthi et al., 2008) are compared with proxy estimates (bottom panel; see Table S1) for the Pliocene Epoch indicated with beige shading. Smoothed curves have been fit to highlight trends in pCO_2 and temperature during the Pliocene.

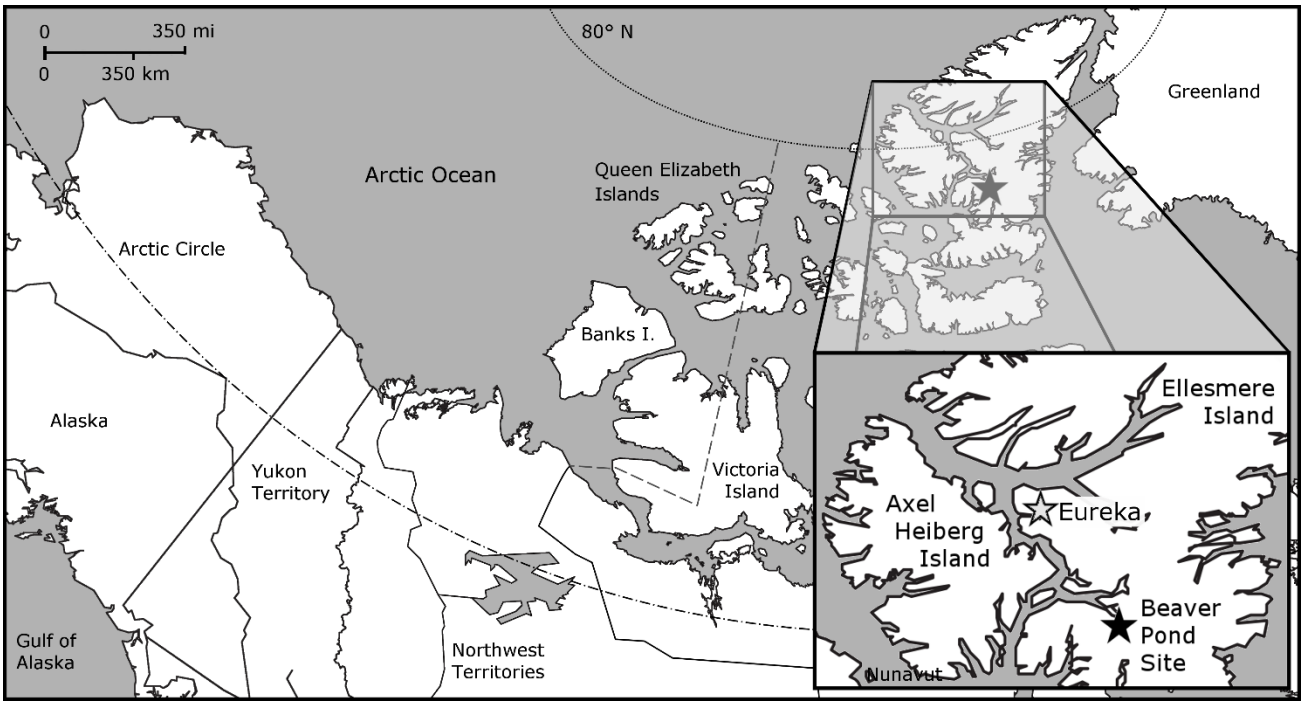

Figure 2. Map of the Canadian Arctic Archipelago, highlighting the location of the Beaver Pond Site (Black Star; 78° 33′ N; 82° 25′ W) and Eureka Climate Station (Grey Star; 80° 13’ N, 86° 11’ W – used for modern climate comparison) on west-central Ellesmere Island.

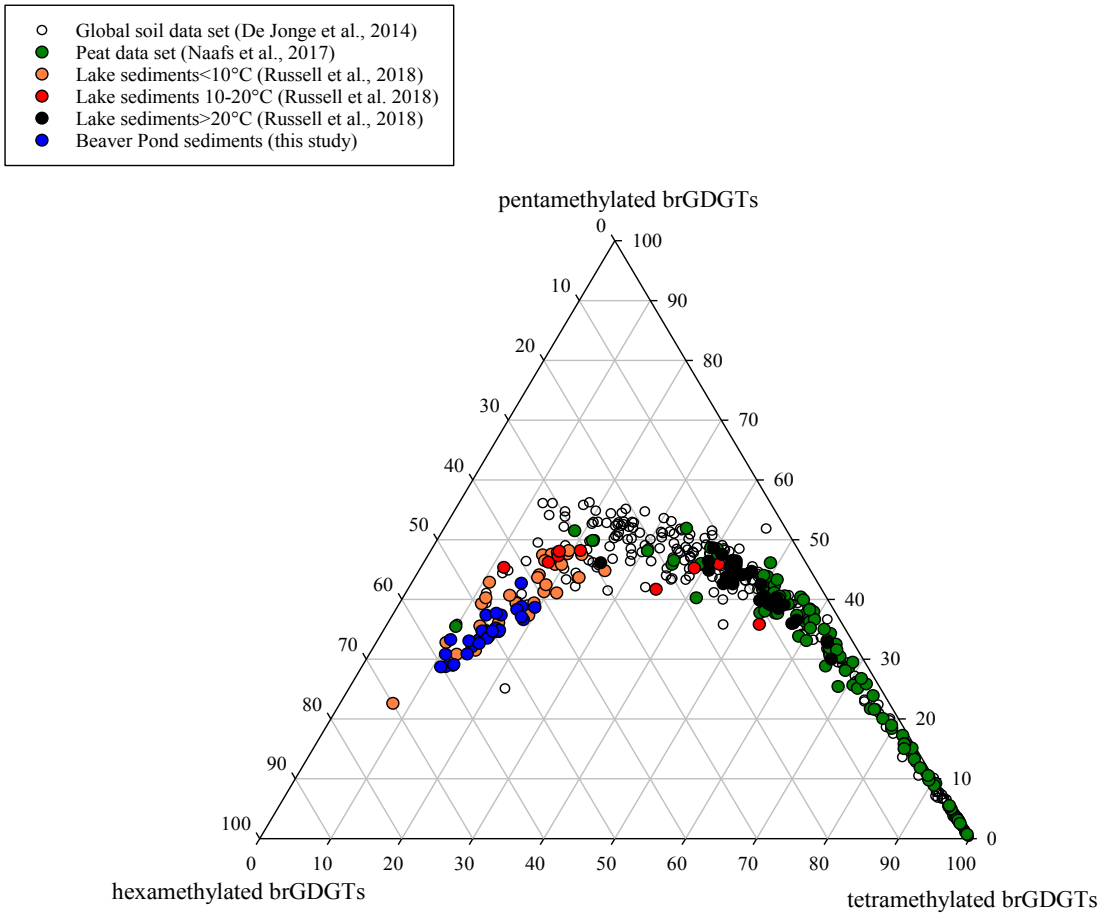

817
818 **Figure 3. A ternary plot illustrating the fractional abundances of the tetra- (Ia-c), penta (IIa-c and II′a-c), and**
819 **hexamethylated (IIIa-c and III′a-c) brGDGTs. The global soil dataset (open circles; De Jonge et al., 2014), the**
820 **global peat samples (green circles; Naafs et al., 2017), and lake sediments from East Africa (black circles**
821 **indicate samples from lakes >20°C, red circles indicate samples from lakes between 10–20°C and orange circles**
822 **designate samples from lakes <10°C; Russell et al., 2018) are included for comparison with the Beaver Pond**
823 **sediments (blue circles; this study).**

824

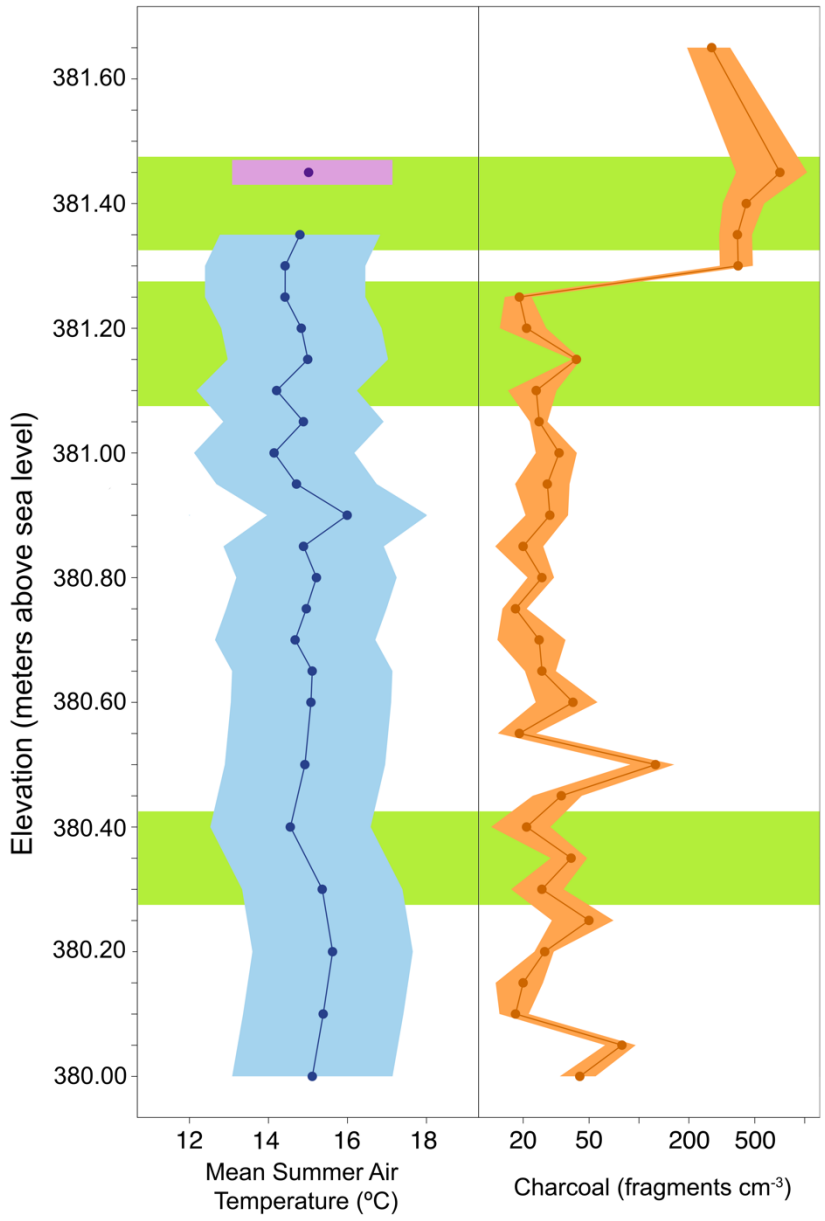

825

826 **Figure 4. Reconstruction of mean summer temperature and fire for the Canadian High Arctic during the**
827 **Pliocene. Mean summer air temperature reconstructed from a brGDGT based proxy (blue; ± 2 σ) and relative**
828 **2010 data point in approximate relative position (purple; ± 2 σ). Charcoal counts reported as the number of**
829 **fragments per volume (fragments cm^{-3}) of peat (Orange ± 2 σ). Green boxes indicate relative depths of pollen**
830 **sampling. Elevation of the deposit is reported as meters above sea level. (Data: Table S3)**

(A)

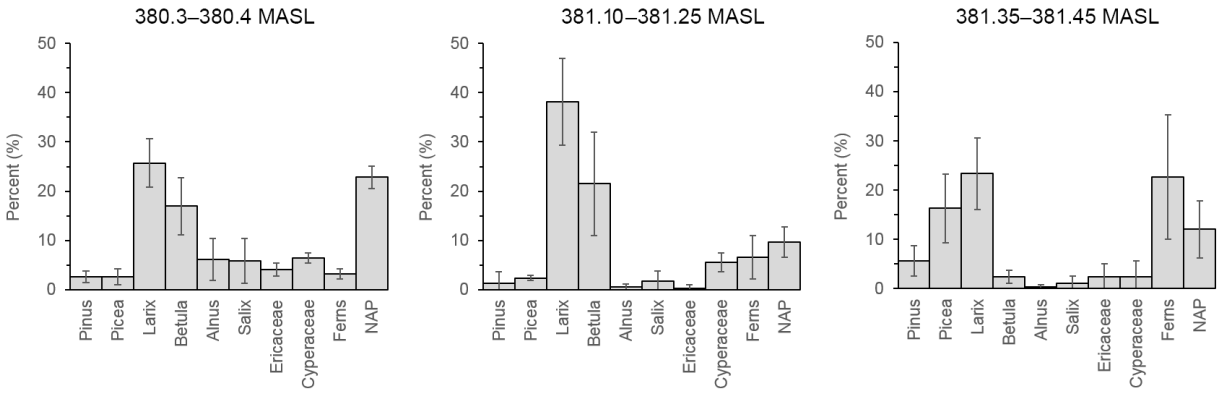

(B)

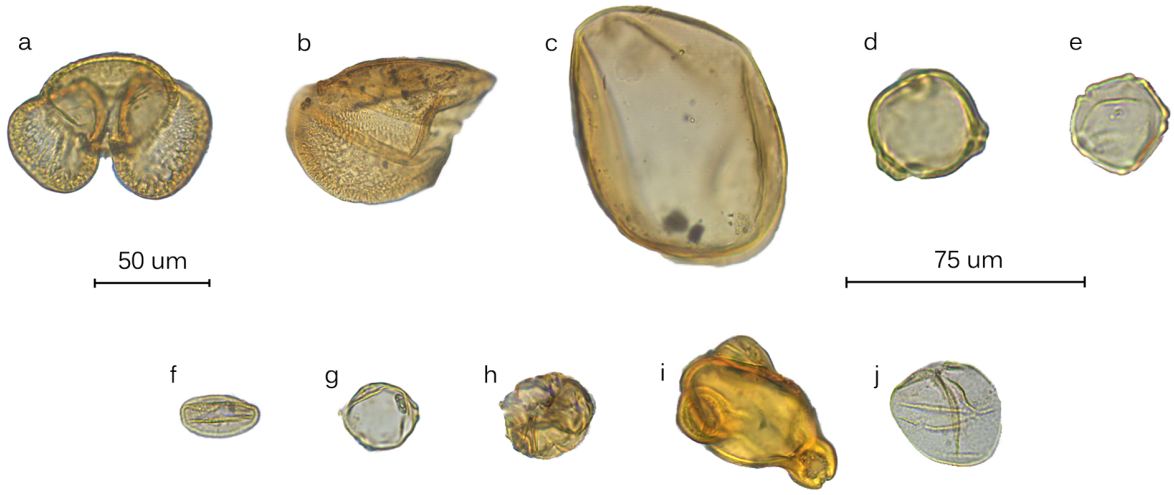

Figure 5. (A) Bar charts showing the relative pollen abundance in each portion of the section (error bars = 95% confidence intervals; MASL- Meters Above Sea Level). (B). Pollen plate of select grains encountered in the BP section: (a) *Pinus*, (b) half a *Picea* grain, (c) *Larix*, (d) *Betula*, (e) *Alnus*, (f) *Salix*, (g) *Myrica*, (h) ericaceous grain, (i) *Epilobium*, and (j) Cyperaceae. 50um scale = (a–c), 75um scale = (d–j).

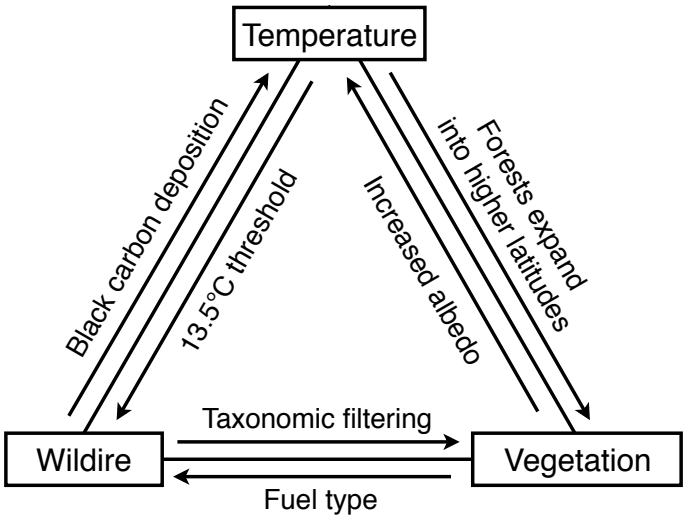

Figure 6: Examples of the feedbacks between temperature, vegetation and wildfire at the Beaver Pond site

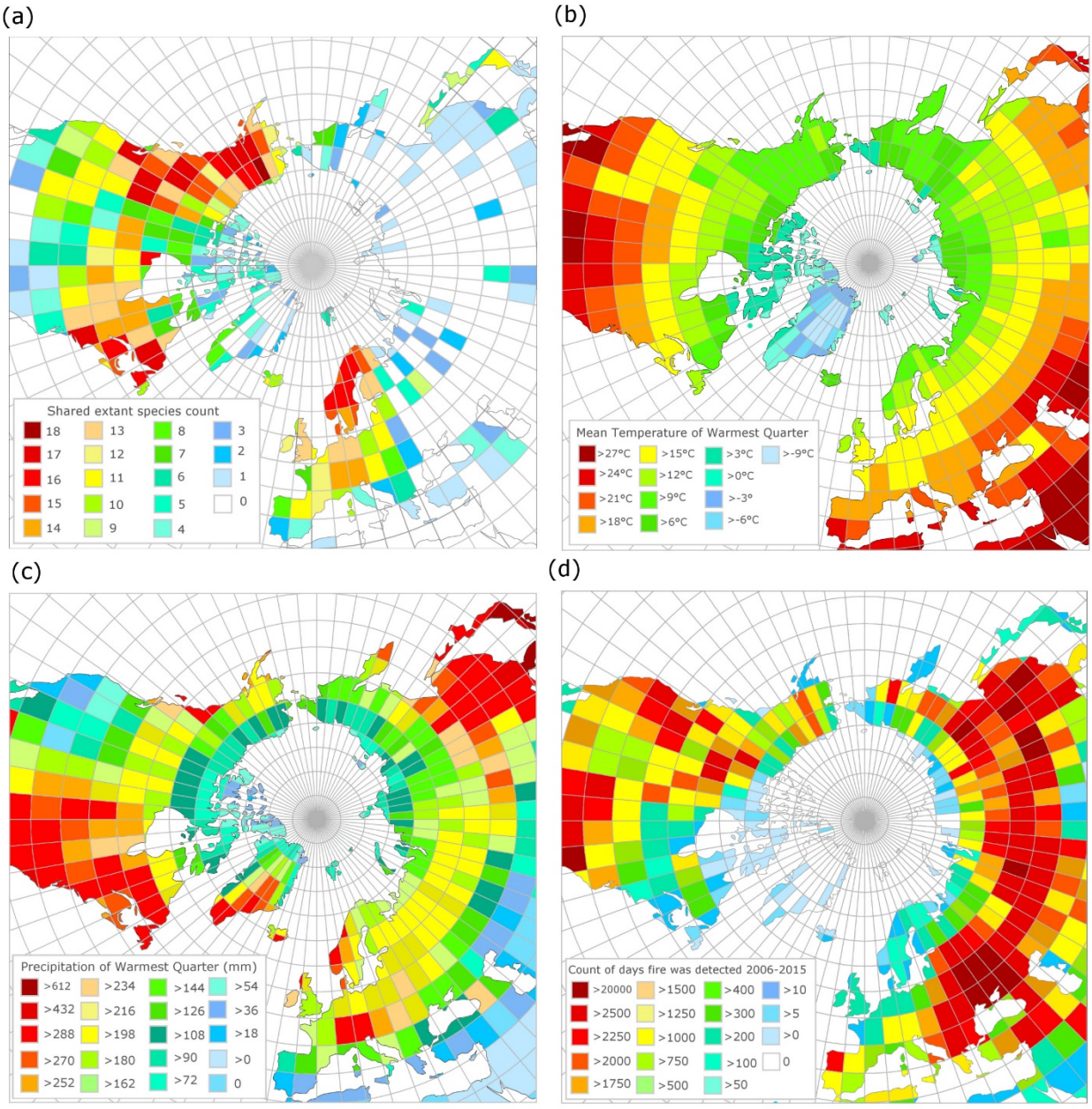

853 **Figure 7. (a) Modern geographic distribution of observed occurrences of species common to the Beaver Pond**
854 **species list, (b) Mean temperature of the warmest quarter (summer average) derived from WorldClim, (c)**
855 **Mean precipitation of the warmest quarter (summer rain) derived from WorldClim, (d) Count of unique fire**
856 **pixels detected per day, over 10 years from MODIS 6 Fire Product, normalized by area of the latitude by**
857 **longitude grid.**

858